School of Computing, Engineering and Mathematics

Division of Engineering and Product Design

Title:

"Investigating the mitigations of the effects wind turbines have on Air Traffic Control"

Author: Hassan Oyelaja

DISCLAIMER

I hereby certify that the attached report is my own work except where otherwise indicated. I have identified my sources of information; in particular I have put in quotation marks any passages that have been quoted word-for-word, and identified their origins.

Signed:

Date: 5/May/2016

Abstract

This project investigates the effects wind turbines have on air traffic control; whilst highlighting the current methods already employed to mitigate these effects, this research study also proposes another potential mitigation measure which is, the implementation of stealth blades in wind turbine design.

Further to the proposition of the stealth wind turbine blades, this project studies the radar cross-section of a scaled conventional wind turbine blade model and compares it to the radar cross section of the proposed stealth wind turbine blade model. This involves the analysis of various factors that contributes to the magnitude of the radar cross-section of an arbitrary target. To ensure the radar cross section predictions were valid for analysis purposes, the simulation software 'Computer Simulation Technology Microwave Studio - (CST MS)' used to simulate the radar cross section of the blades was validated using underlying principles and the basic hypotheses that govern radar cross section prediction for different objects.

Ultimately, recommendations regarding the best method of mitigating wind turbine effects on air traffic control are provided based on the research and analyses presented in this project.

Contents

Table of Figures

Table of Equations

Acknowledgment

I would like to show my appreciation to a number of individuals within the University of Brighton as well as at the National Air Traffic Services (NATS) for their support during this project.

Firstly, I want to thank Dr Dal Koshal for his advice, support and guidance during this project and throughout my industrial placement year.

Secondly, I would also like to thank Sacha Rossi; my technical manager during my placement year at NATS for providing me with the platform to explore this topic.

Further appreciation goes to my former colleagues at NATS; Nick Young, Alastair Auld and Colin Sivyer for providing me with expert advice on this subject area as well as Tony Brown for assisting me with my wind tunnel testing.

Finally, I would like to express the highest gratitude to my loving parents (Mr and Mrs, Oyelaja) for their extensive financial support throughout the course of my degree.

Glossary

Word	Abbreviation	Definition
Air Traffic Control	ATC	This is a ground-based service aimed at preventing collision of aircrafts. The main purpose of ATC is to organize and expedite the flow of air traffic.
Air Traffic Control Operator	ATCO	This is an individual who operates various ATC systems e.g. radar displays.
Computer Simulation Technology Microwave Studio	CST MS	Simulation software used for electromagnetic simulation e.g. RCS prediction.
Decibel	dB	Logarithmic unit used to measure power ratio.
Decibel square meter	dBm2	Power ratio relative to one square meter.
Electromagnetic wave	EMW	Synchronized electrical and magnetic fields that propagate at the speed of light.
Hertz	Hz	Unit for wave frequency.
Lossy		A material that absorbs EMW e.g. RAM.
National Air Traffic Services	NATS	UK's main ATC service provider.
Perfect Electric Conducting	PEC	Totally reflects all incident EMW.
Radio Detection And Ranging	RADAR	Radars is used to detect targets e.g. aircraft with the use of EMW.
Radar Absorbent Material	RAM	Main purpose of RAM is to absorb EMW, and make the respective target stealth to radar.
Radar Cross Section	RCS	This is the effective radar signature of a target, Unit in DB2M or Meter squared.
Wind farm		A geographical region where wind turbines are located.

Project structure

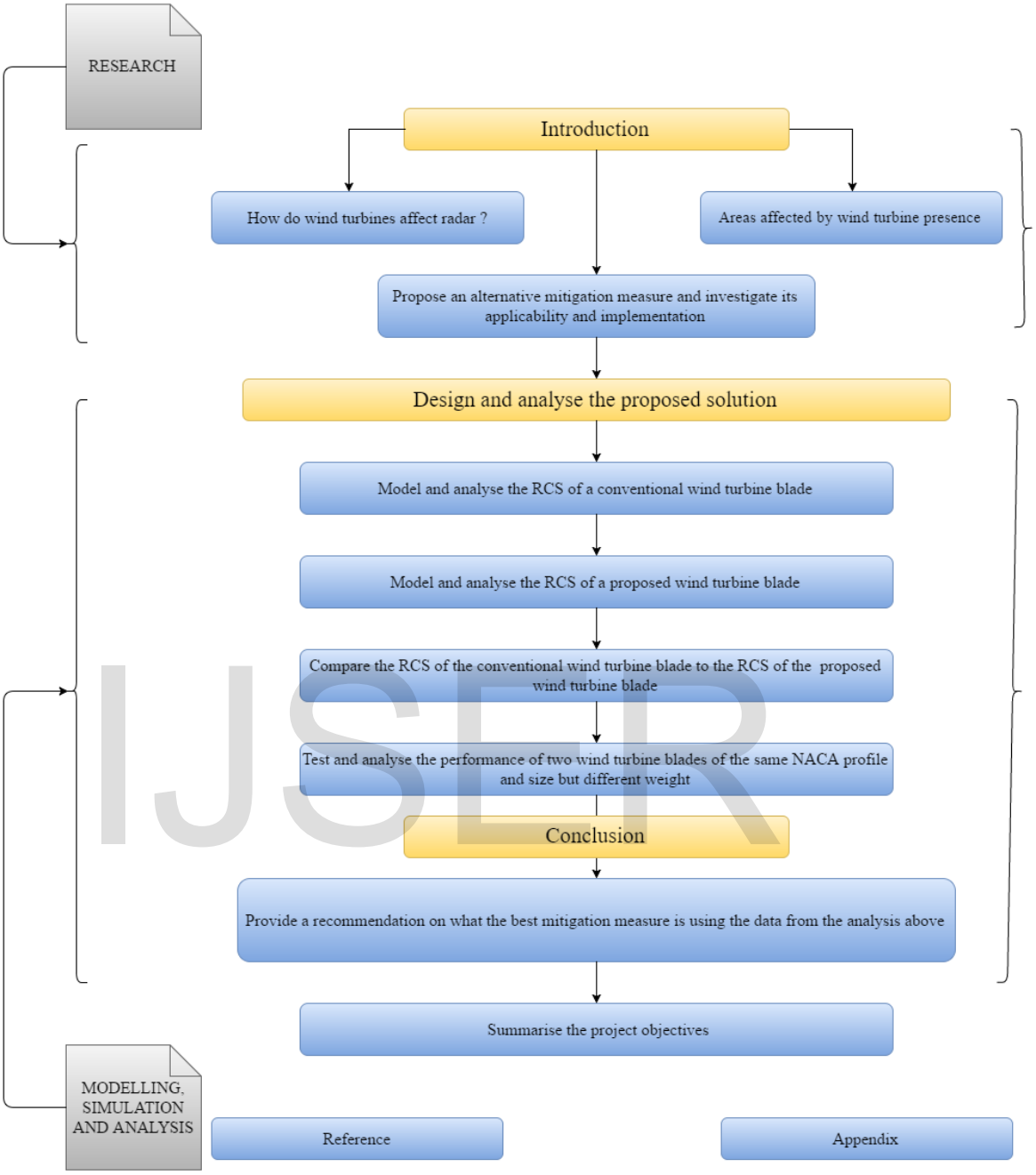

Figure 1 - Project structure

Chapter 1

Introduction

The debate on how the world will thrive with the dwindling reserves of non-renewable energy has been the focal point of innumerable academic journals, scientific reports, symposiums, and researches. Although newer technologies have been adopted in this field to curb this increasing problem, the field of non-renewable energy still remains a crucial, but challenging field that still requires extensive research to solve this budding question. Hence, driven by growing external global pressures and forces, researchers have now been focusing their efforts into alternative sources of renewable energy such as wind energy that is extracted mainly using wind turbines.

Wind turbines have the advantage of harnessing a substantial amount of wind power that can be used for everyday needs. However, as with all forms of technological solutions, wind power is not impervious to unforeseen issues. A prime example of this can be seen in that their presence in certain locations has been reported to **severely affect the effective functionality of *Air Traffic Control (ATC) radars***. According to NATS (2015), further problems reported include reduced sensitivity and overloading of processing functions, as well as the degradation of voice communications facilities and en-route navigation aid; *but how do they affect radar?*

1.1 The principle of radar operation

A simple radar sensor consists fundamentally of a directional antenna, an RF (Radio Frequency) transmitter and a receiver followed by a processor and a display (Illustrated in Figure 2). Using the antenna, the radar transmits a pulse of electromagnetic energy in a specified direction, upon interference with an object, a portion of the energy is reflected back to the antenna as a signal containing information, which is then amplified and processed before being displayed as a target image.

The range/distance *r* of the interfering object/target from the radar is determined based on the measured time taken for the electromagnetic wave to travel to and fro the object e.g. Aircraft (Illustrated in Figure 3)

$$Speed\ of\ electromagneticwave = \frac{Distance}{Time}; where\ speed\ of\ electromagnetic\ wave\ equals\ speed\ of\ light$$

Equation 1 - Motion equation

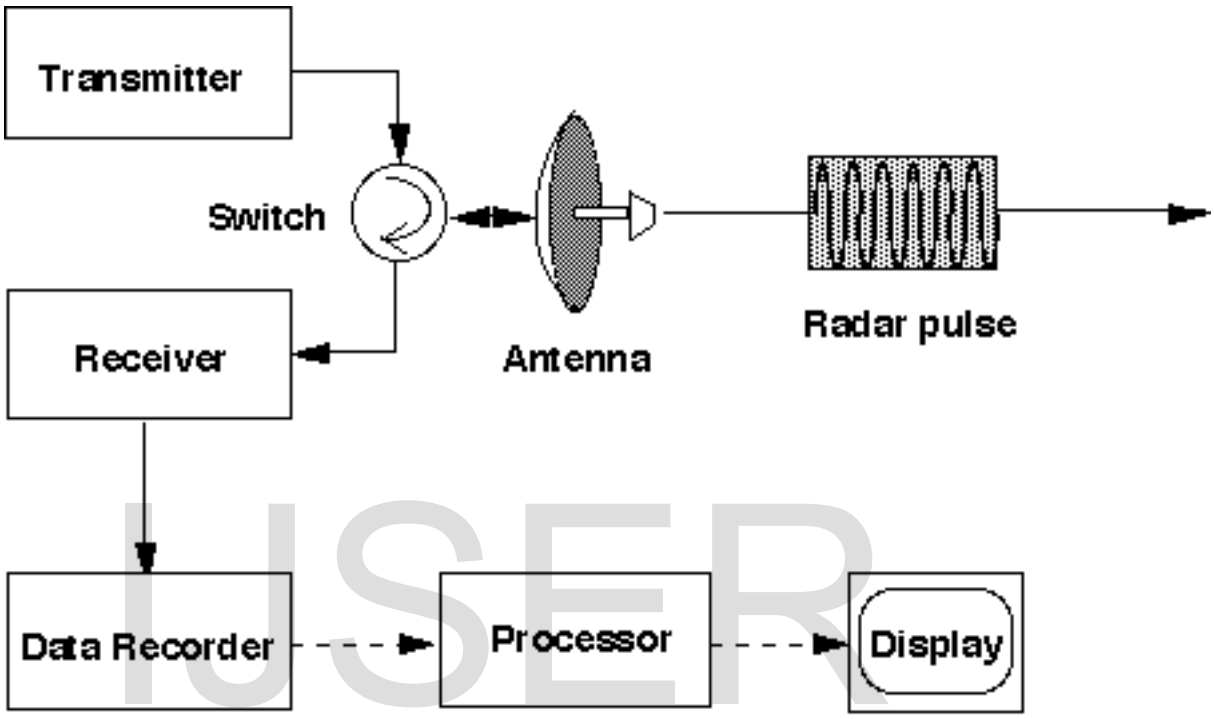

Figure 2 - Schematic of a conventional radar operation (Radar concepts | ECE 480 team 5: Interactive radar demonstration, 2014)

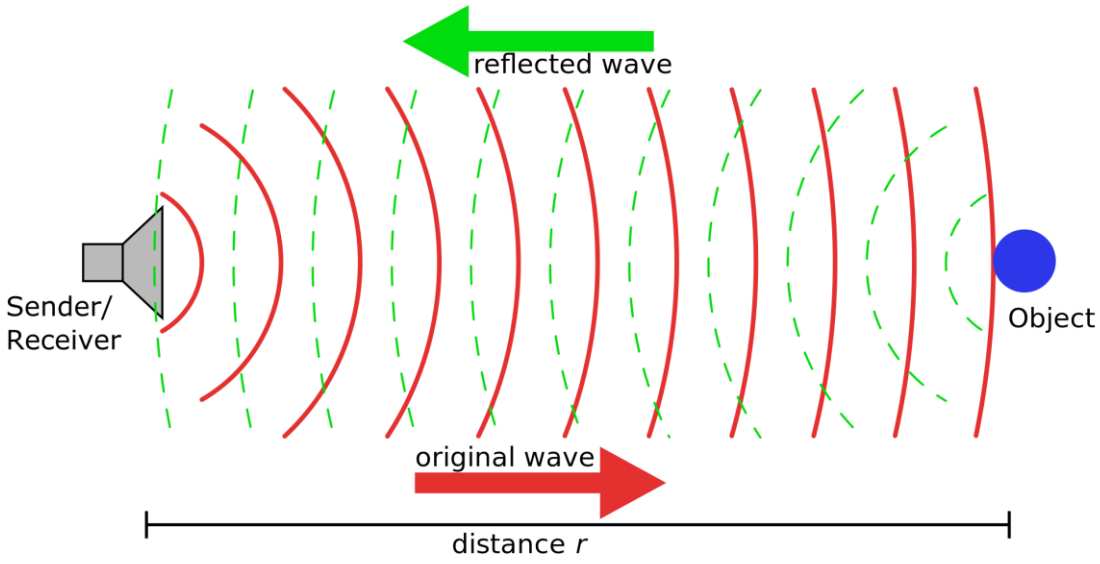

Figure 3 - Distance travelled by transmitted and reflected wave (O'Donnell, 2002)

1.2 How wind turbines affect air traffic control radar

A wind turbine consists of three main elements, the assembly of the blades, nacelle and the tower.

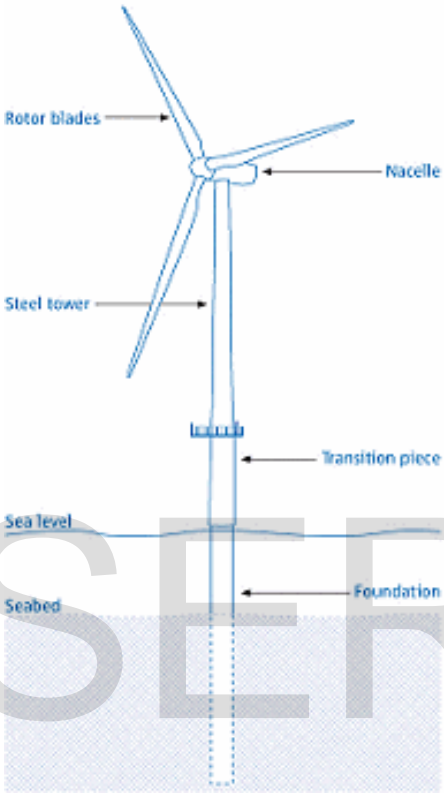

Figure 4 - Typical wind turbine structure (Fleseriu, 2014)

These features, if within the sight of a radar, they reflect electromagnetic wave back to the radar resulting in the following consequences:

- High reflections may cause amplitude limiting within the signal processor or receiver thus resulting in the desensitization and reduced detection of aircrafts within the area NATS (2015).
- Air traffic controllers are unaware of this desensitization and consequently, this results in them missing aircraft responses.
- The movement/rotation of the turbine blades imposes a **Doppler Effect** on the reflected signal. Doppler processing is used by majority of radars to distinguish

between stationary and moving objects. The radar perceives the Doppler effects produced by wind turbine blades and aircrafts as similar; hence it is unable to differentiate between the Doppler Effect imposed by a moving aircraft and the Doppler Effect imposed by the moving blades of the wind turbine. The concept of Doppler effect is explained further in (Section 2.1 Understanding Doppler Effect)

- A confused image is displayed to the Air Traffic Control Operator (ATCO) declaring both wind turbines and aircrafts as moving objects (Illustrated in Figure 12)

This project seeks to identify what initiatives need to be undertaken in order to mitigate the above effects wind turbines have on air traffic control (ATC)

The first part of this report will highlight in more details the current technical issues posed by wind turbines on air traffic control radar; this section will discuss the current mitigations already in place and also provide another potential mitigation measure that could be implemented in the long term.

This project will then look further into the analysis, design and implementation of the highlighted potential mitigation measure to this issue. The latter section of the report will contain various mathematical calculations, engineering simulations and modelling of the highlighted potential solution.

Furthermore, this project will also compare the proposed mitigation measure to the already existing solutions, highlighting the novelty of the proposed measure. In the same vein, the concluding part of this report will summarize what the best short term and long-term solutions are to ensure the symbiotic existence of wind turbines within the sight of air traffic control primary radars.

1.3 Aim of Project

To investigate what initiatives should be undertaken to mitigate the effects wind turbines have on air traffic control.

1.4 Objectives of Project

1. Identify what the cause of the issue is and investigate the current solutions.
2. Identify the areas that are currently affected by the presence of wind turbines.
3. Propose an alternative mitigation measure, identify its practicality and determine its applicability and implementation.
4. Design and analyse the proposed mitigation measure:
    4.1 Model current conventional wind turbine blade and analyse its Radar Cross Section (RCS).
    4.2 Model proposed wind turbine blade using stealth principles and analyse its radar cross section.
    4.3 Compare the RCS of the proposed stealth wind turbine blade to the conventional wind turbine blade.
    4.4 Analyse how the implementation of Radar Absorbent Materials (RAM) will affect the efficiency of a wind turbine blade.
5. Provide recommendation on what the best mitigating measure is using data from the above analyses.

This page is intentionally left blank.

Chapter 2

Background

Objective 1: Identify what the cause of the issue is and investigate the current solutions.

As wind turbine developments have proliferated over the years, the current mitigations imposed by air traffic control organisations to reduce its effects on air traffic service operations have not been sufficient due to various reasons.

The following are the mitigation measures currently in place to combat the effects of wind turbine effects on radar.

a) Blanking

This process involves blanking out geographical areas where wind turbines exist within the line of sight of the radar, out of the radar system, i.e., no radar output from the affected airspace above that geographical region will be displayed to the air traffic control operator (Illustrated in Figure 13). As the number of wind turbines being built is growing rapidly, this will no longer be a viable mitigating measure because blanking out numerous airspace above these geographical regions (wind farms) out of the radar will reduce the effective areas that are actually under the radar's surveillance. Furthermore, the restriction imposed by the Civil Aviation Authority (CAA) on Air Navigation Service Providers (ANSP) is that *'an ATC radar must see at least 90% of the targets within its coverage range' (CAP 670: ATS safety requirements, 2014)* thus making *'blanking'* a non-viable mitigation measure for the long term because wind farm developments are growing tremendously.

b) Pre Planning Assessment

Before the commencement of a wind farm project, that is, before a wind farm development/building process takes place, various pre planning assessments have to be carried out, one of which includes checking if a potential wind farm will affect radar; this is a preventive method taking by the National Air Traffic Services (NATS) to predict the effects a potential wind farm would have on the nearby radars.

Oyelaja, H. (2015) demonstrates how wind turbine pre planning is carried out in a video (See reference list).

- **Comparing radar coverage at 40meters and at 200meters above ground**

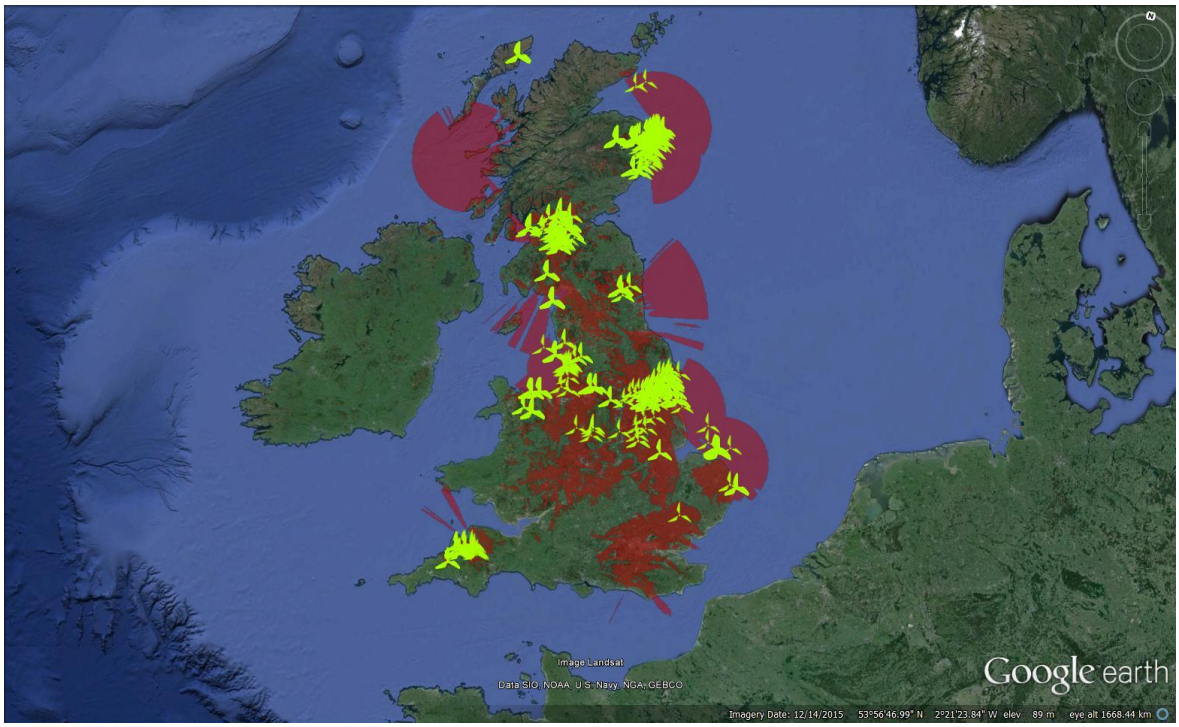

Figure 5 - Wind turbine dispersion across UK and Radar coverage at 40 meters *Oyelaja, H. (2015)*

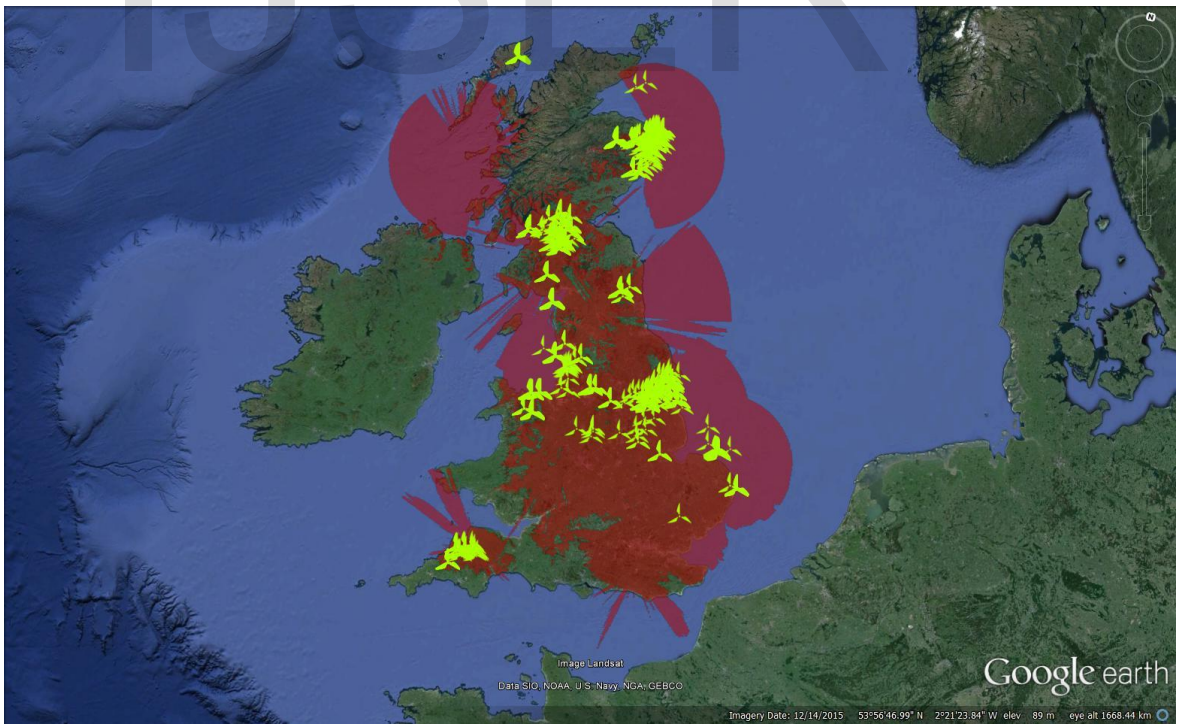

Figure 6 - Wind turbine dispersion across UK and Radar coverage at 200 meters *Oyelaja, H. (2015)*

Figure 7 - Close up image showing 'Wingate' wind turbines (Green Icons next to turbines) *Oyelaja, H. (2015)*

Figure 5 and Figure 6 show the radar coverage at different heights above ground, **the red marked areas** are regions visible to radar at that specific height. Clearly, there are more red marked areas at 200 meters, this is because less buildings/physical structures are interfering with the radar radiations at 200 meters than at 40 meters above ground.

The **green icons** show various consented built wind turbines across the UK, this implies wind turbines currently in place that affect radar. NATS 2015, consented and allowed these wind turbines to be built because they could be and are currently being mitigated by **blanking.**

From Figure 6, wind turbines above 200 meters high and fall within the red marked zones will interfere with radar, this is the same at 40 meter (i.e. - wind turbine as high as 40 meters and fall in the red marked zones in Figure 5 will be seen by radar). This is the case at all other heights if the radar coverage at that height is known.

c) Project RM

Study shows that the effects wind farms have on ATC can be mitigated by either redesigning the wind turbines to make them stealthy to radar or by enhancing radar data processing to enable a more efficient processing of wind turbine electromagnetic wave reflection.

Over the years, various radar improvement have been made to help with this issue, a major improvement includes the deployment of **Project RM.**

Project RM provides wind turbine mitigation in a scalable and sustainable way, it provides enhancement to the radar system by reducing wind turbine effects in certain airspace. Wind turbines in line of sight of Project RM equipped radars outside 9 nautical miles from the radar head, where the vertical angle between the base of required coverage and the turbine tips is 1.2 degrees or greater measured from horizontal can be mitigated, thus providing uninterrupted coverage over the wind farm. NATS (2015)

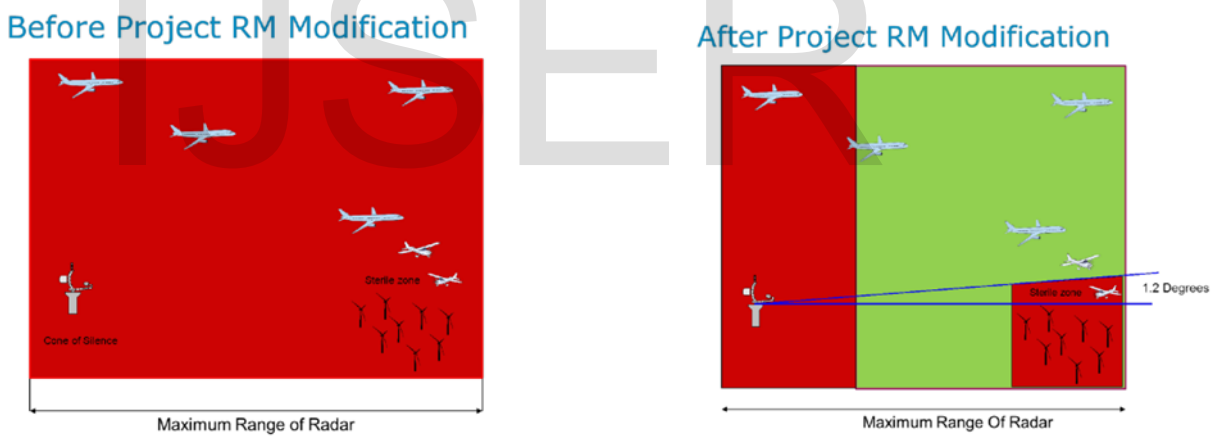

Figure 8 - Illustration of the mitigating effect of Project RM (NATS, 2012)

Green area shows where aircrafts can be seen, Red area show where aircrafts cannot be seen.

Although Project RM was successful in creating a scalable solution to wind farm effects; this is not sufficient. In recent years, the wind turbine mitigation industry is becoming more inclined towards implementing various stealth technologies in wind turbine developments (Techxplore, 2014).

Stealth technology is a sub-discipline of military tactics that covers a broad range of techniques used to make fighter aircrafts less visible to radar. Some of these techniques include defining the **shape** of military air vehicles in forms that **deflect electromagnetic radiations** away from the radar receiver, coating chassis of air vehicles **with Radar Absorbent Material (RAM)** to allow radar energy to be absorbed and converted into heat; thus ideally not reflecting any energy back to the radar receiver (Defense-Aerospace, 2014)

Various firms such as 'QinetiQ and Vestas Wind Systems' have then looked to implement this knowledge into the design of wind turbines blades; QinetiQ – a consultant and technology provider to the energy and environmental sectors – and Vestal Wind Systems – A market leader in the supply of wind power solution.

Both firm recently collaborated in a five-year project to deploy the world's first stealth wind turbine blades; these blades have successfully passed various trials. Stealth turbine blades look to be the future of mitigating the effects of wind farm on air traffic control. (QinetiQ, 2009)

2.1 Understanding Doppler Effect

Doppler Effect is a change in frequency when a sound source moves either towards or away from the listener, or when the listener moves either towards or away from the sound source. This principle, discovered by the German physicist *Christian Doppler*, applies to all wave motion; e.g. radar wave transmitted to and reflected from an aircraft (LCDR Brent J. Flaskerud, 2006)

Doppler's effect is an essential phenomenon used by radar systems to perform target filtering; i.e., distinguish between **stationary and moving objects** e.g. building, birds, trees; but as the rotating blades of a wind turbine produces similar Doppler effects as aircrafts, filtering wind turbines out of the radar output cannot be done using this technique, thus the unwanted returns from wind turbines are not filtered out by the radar system, this in turns severely affects the effective functioning of the ATC radar.

Doppler effect can primarily be explained using this simple analogy; when a vehicle is moving toward you, the sound wave from the vehicle increases as it gets closer, and vice versa when a vehicle is moving away from you, the sound wave decreases.

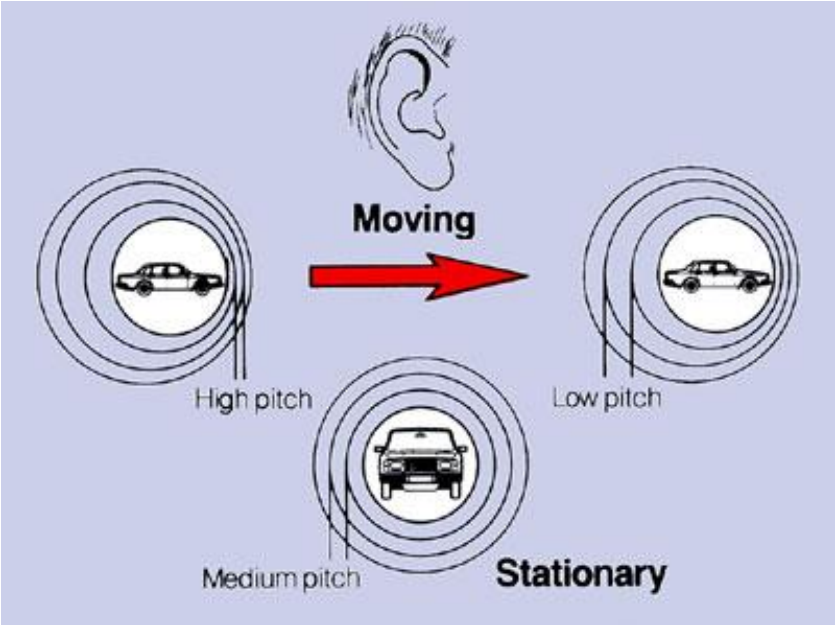

Figure 9 - Doppler Effect: Illustrating the difference in frequency between a stationary and moving vehicle (ECHO, 2006)

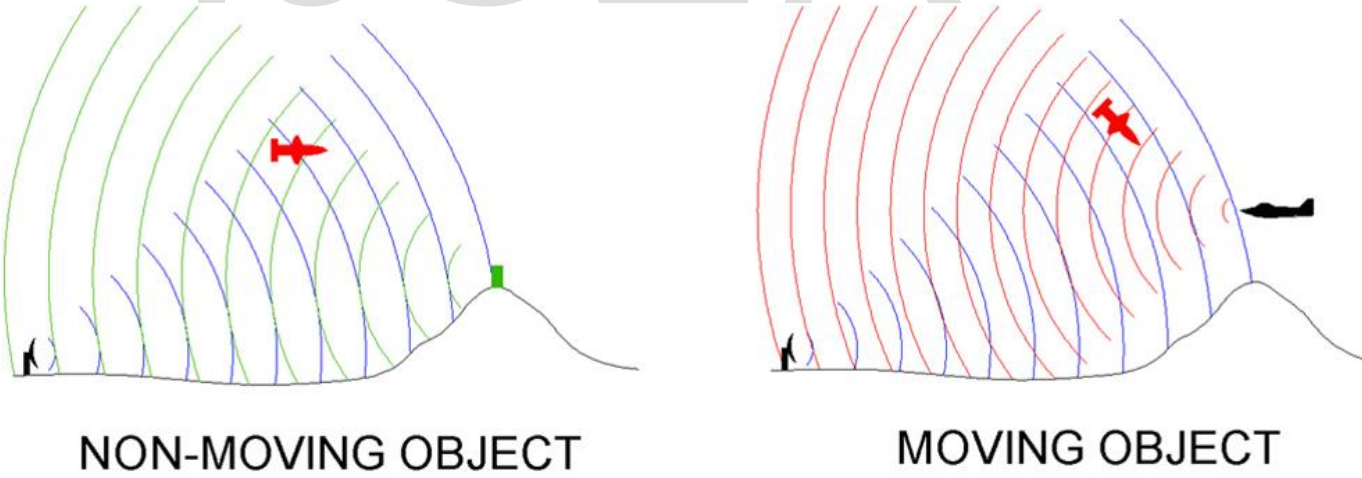

Figure 10 - Doppler Effect: Illustrating the difference in frequency between transmitted and received waves for moving and non-moving targets (Phillip R. Hays 2009*)*

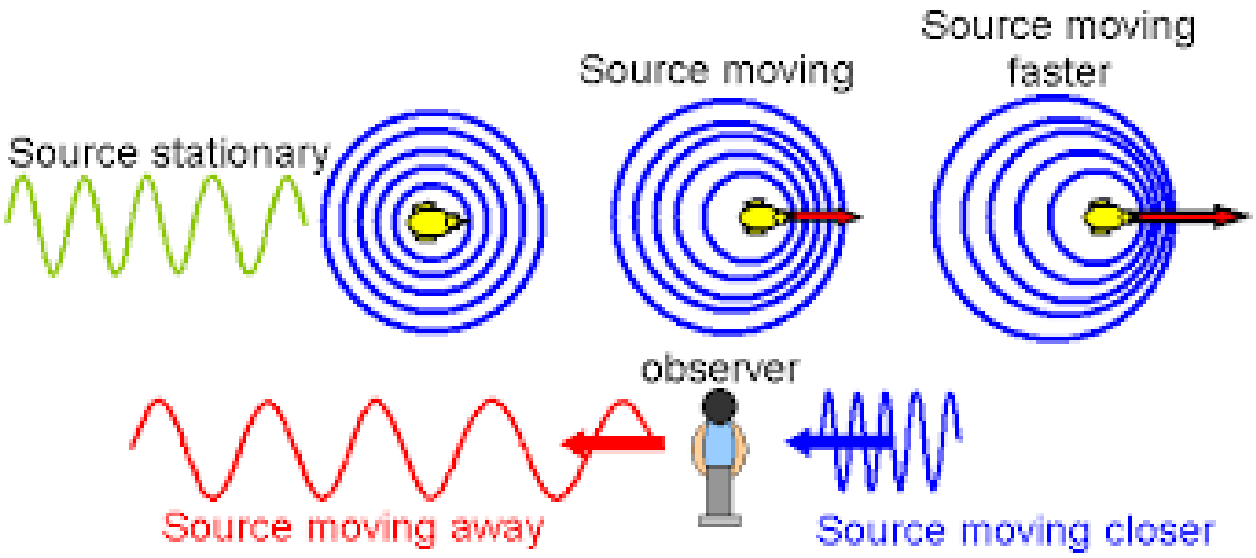

Figure 11 - Doppler Effect: Illustrating the difference in frequency between an object moving away from an observer, moving towards an observer and a stationary object (Hodgkins, 2009)

This is how a radar distinguishes between a stationary and a moving object using the Doppler's effect.

*Notice, there is a change in the frequency of a wave reflected from a moving object, i.e., in the case of detecting aircrafts. Wind turbines produce similar Doppler Effect as aircrafts. So filtering out wind turbines using this method could in turn filter out real aircraft target.

In Figure 12, *(Left)* shows an air traffic operator's screen with wind turbine *(Right)* with wind turbine but with some form of radar mitigation.

The picture on the *left* is as a result of the Doppler clutter from wind turbines in that location, the radar system does not filter these returns out as it assumes they are aircrafts.

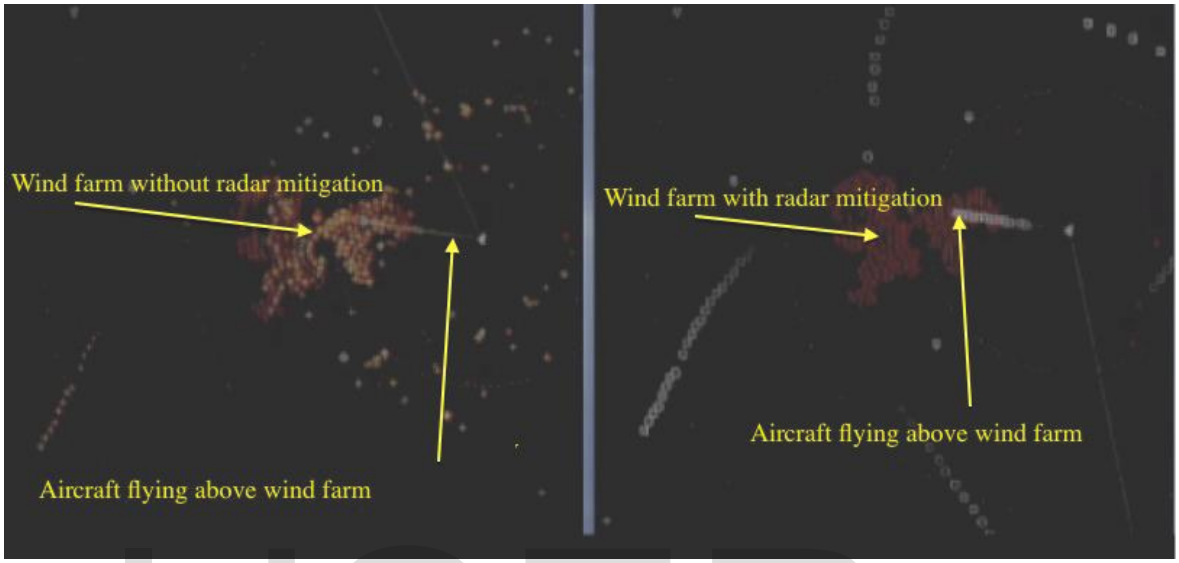

Figure 12 - Clutter on radar screen

From the picture above, the **orange dots** in the middle of the *left screen* represents a **wind farm**, it is noticed that the aircraft's track is lost as soon as it enters the wind farm, the picture on the *right* shows the aircraft is still been tracked across the wind farm after a mitigation measure has been implemented **(Aircraft tracks are in white).**

As explained previously, another method used to mitigate wind farm effect on air traffic control radar display is *blanking*; this is when all radar output over a wind farm is filtered/blanked out of the screen of the Air Traffic Control Operator (ATCO) (Illustrated in Figure 13). Although coverage is lost in that vicinity, the ATCO navigates aircrafts around the blanked zone to prevent loss of target, that is, the aircraft being navigated, preventing a situation where by the aircraft being controlled flies into the blanked zone.

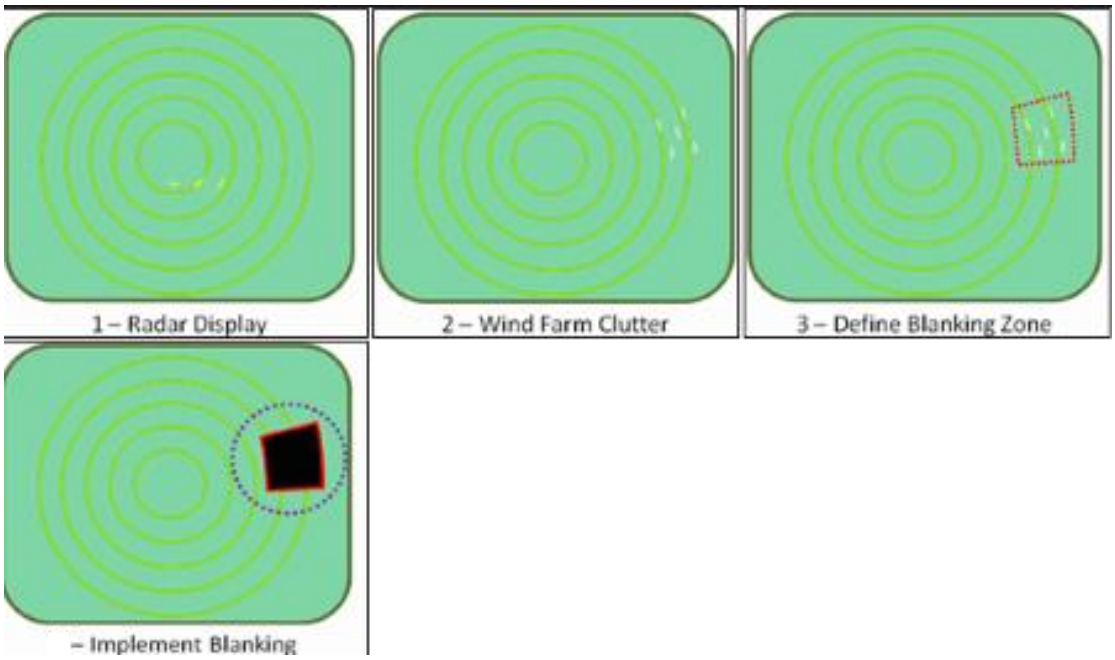

Figure 13 - Illustration of how a blanked area on a radar display appears to an Air Traffic Control Operator (Frolic, 2013)

*Note - As a result of these wind turbine issues with ATC, the safety of aviation is being compromised; hence, various wind farm development projects have been halted.

NATS, (2015) *UK's air navigation service provider* holds about 2.2 Gigawatts of electricity in objections to wind farm development within the vicinity of air traffic control operations, with this reason, this project looks to investigate the practicality of reducing wind turbine effect on air traffic control in order to allow the continual growth of wind energy developments; one of the ways this will be done is through the reduction of the Radar Cross Section (RCS) of wind turbine blades.

The methodology of RCS prediction, for example in stealth aircrafts is explained in section 3.1 Principle of Stealth. In the same vein, this project will propose a new design for wind turbine blades taking into consideration the factors outlined in Section 3.2 Radar Cross Section (RCS) as well as analyse the RCS of the proposed stealth wind turbine blade.

The **radar cross-section (RCS)** of a target is the effective area intercepting an amount of incident power which, when scattered in an isotropic manner generates a level of reflected power at the radar equal to that from the target.

Radar cross section is measured in dBm2 that is., decibels relative to one square meter- this is a function of the geometry, material of the target of interest etc. (see Section 3.2Radar Cross Section (RCS)).

2.2 Areas currently affected by wind farms

Objective 2: Identify the areas that are currently affected by the presence of wind turbines.

There is an abundance of wind farms across the UK and with this immense dispersion, a number of wind turbines in certain locations currently affect the effective functioning of air traffic control services (radars) as explained previously.
Although some of the effects caused by the presence of certain wind farms can and have been mitigated to an extent, the wind turbine policy imposed by (NATS,2015) stops further development of wind farms in locations that could have potential effects on air traffic control operations.

The statistics below shows the number of wind turbines across the UK.
As these figures only represent wind farms within the UK, it does not reveal the extent to which wind turbines affect air traffic control on a global scale.

2.2.1 Wind turbines across UK

Wind Turbine	Number	Capacity MW/h
Onshore	5140	8347
Offshore	1450	5048
Total	**6590**	**13395**

2.2.2 Wind turbine project refusals

Project	Project Number	Capacity (MW/h)
Onshore	1103	9188.371
Offshore	2	1510
Total Capacity	**1105**	**10698.371**

Figure 14 - UK Wind farm statistics as of 21/11/2015 (RenewableUK, 2015)

Of the total capacity of approximately 10.698GW of potential power that could be produced by the halted wind turbine projects; air traffic control contributes about 2.2GW; that is, wind turbine development/projects that could produce 2.2GW of electric power have been objected/halted by UK's air navigation service provider as a result of the potential effects these wind farms could have on air traffic control radars (NATS, 2015)

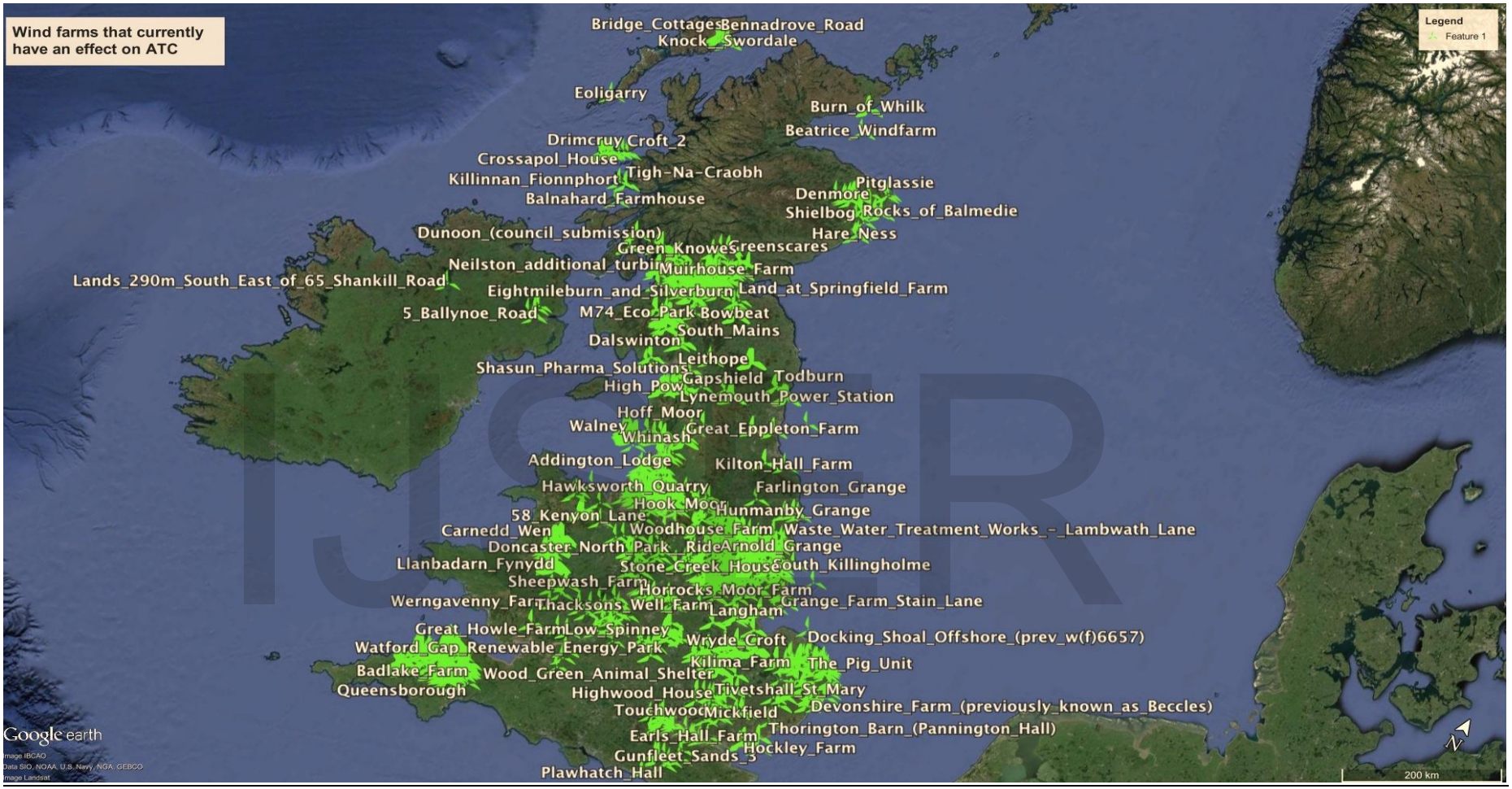

Figure 15 - The satellite image shows the wind farms that are currently under some form of radar mitigation as a result of their effects on air traffic control (Oyelaja, 2015)

2.3 Case Study

Walney wind farm

This is an offshore wind farm with wind turbines about 200 meters high; at this height, the wind turbines in this wind farm are within radar coverage, and as explained in Section 2.1

Understanding Doppler Effect, the respective radar experiences a confusion in the Doppler processing generated from this wind farm as the wind turbines are interpreted as moving objects by the radar; thus resulting in a clutter on the radar screen (see Figure 12).

The current mitigation put in place is the ‘blanking’ of ‘Walney wind farm’ so no radar data is processed from that geographic region, this blanking mechanism results in aircrafts being forced to be navigated away from the blanked region (Airspace above Walney wind farm) to avoid them being lost in the wind farm clutter, that is, any tracks of aircraft flying in the airspace above ‘Walney wind farm’ will be lost amongst the wind turbine clutter.

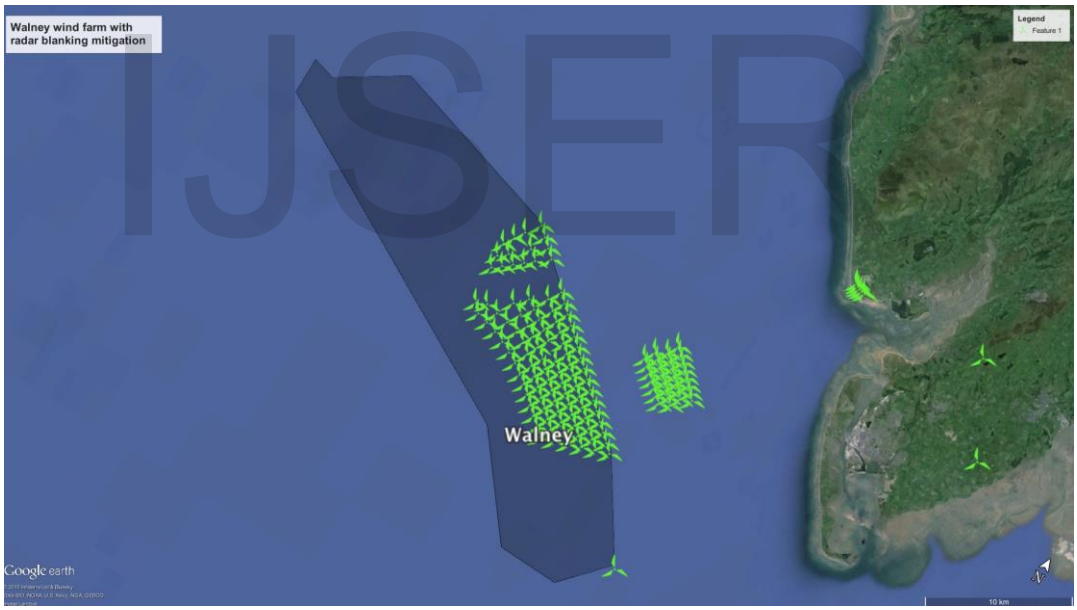

Figure 16 - The satellite image of Walney wind farm; green icons represent a single wind turbine (Oyelaja, 2015)

The ‘blanking’ mitigation technique is the most common method currently in place to combat the effects wind farms have on air traffic control radar; hence a number of wind farm that pose an effect on ATC as illustrated in Figure 15 have been blanked out of the radar system output.

As specified by the Civil Aviation Authority, 2014, *“a functional air traffic control radar must see 90% of the target within its coverage range”;* this has thus made blanking as a method of wind farm mitigation unviable for long-term purposes.
Wind turbine developments are growing thus blanking out every airspace with wind farm present will result in a reduction of the effective coverage of the radar; thus compromising the functional safety and integrity of the radar.

This page is intentionally left blank.

Chapter 3

Further research and proposal

Objective 3: Propose alternative mitigations, identify the most practical solution and determine its applicability and implementation.

Other mitigation measures developed and implemented by various air navigation service providers around the world include enhancing radar signal processing; typical example is *Project RM* - a mitigation technique developed by the National Air Traffic Services UK, the principle of operation of project RM is explained in the *background section* of this report.

Some other developments to radar data processing also include but are not limited to: Range and Azimuth Gating (RAG), Sensitivity-Time-Control (STC), Use of secondary radar plots, Track initiation inhibit.
These are enhancements made to the radar systems and although they are beneficial, they have not proven sufficient to tackle this problem; it is worth noting that the solution to this problem may lie in the physical design and construction of the wind turbine structure itself other than just an improved radar data processing, this is what this project investigates.

To assess how the physical structure of a wind turbine affects its visibility to radar (radar signature), we will look at the principle of stealth in a fighter jet as this presents a similar approach to the relationship between the design of a physical structure and relative radar signature.

3.1 Principle of Stealth

This section will look at the principles of stealth technology and how these principles can be implemented to the design of a stealth wind turbine, that is, one that would have a low radar cross section (less visible to radar).

Firstly, we need to understand what stealth is; also, the study of the stealth properties of a fighter jet will be imperative.

Henceforth, we will look at a sophisticated stealth aircraft the 'F-117 Nighthawk'

3.1.1 Principle of Stealth in an F-117 Nighthawk

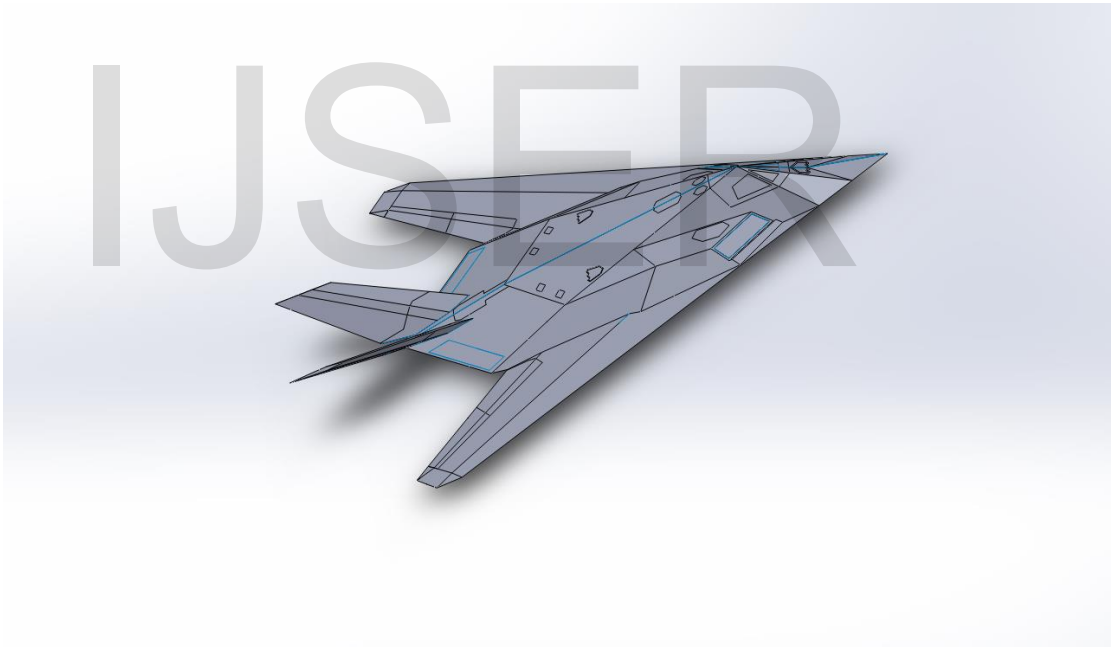

Figure 17 - Solidworks: 3D rendering of an F11-Nighthawk illustrating the relatively angled chassis (CAD library, 2012)

What makes this aircraft stealth? From the 3D Solidworks model above, it can be noticed that the relatively angled chassis of the aircraft allows for an **effective deflection of radar electromagnetic wave** away from the radar receiver, this shape encourages scattering of the incident wave form from the radar; thus little or no energy is reflected back to the radar, the radar cross-section of this aircraft is relatively low thus ideally making it invisible to the radar.

The body of this aircraft is manufactured with a sheet of **radar absorbent material (RAM)**, RAM does not reflect radar wave, it **absorbs the radar energy** and converts it to **heat energy**; this is also an effective technique the F-117 Nighthawk also employs to reduces its' visibility to radar.

3.2 Radar Cross Section (RCS)

This is the effective **radar signature** of a target, a number of factors affect the magnitude of the radar cross-section of a target, and they are as follows:

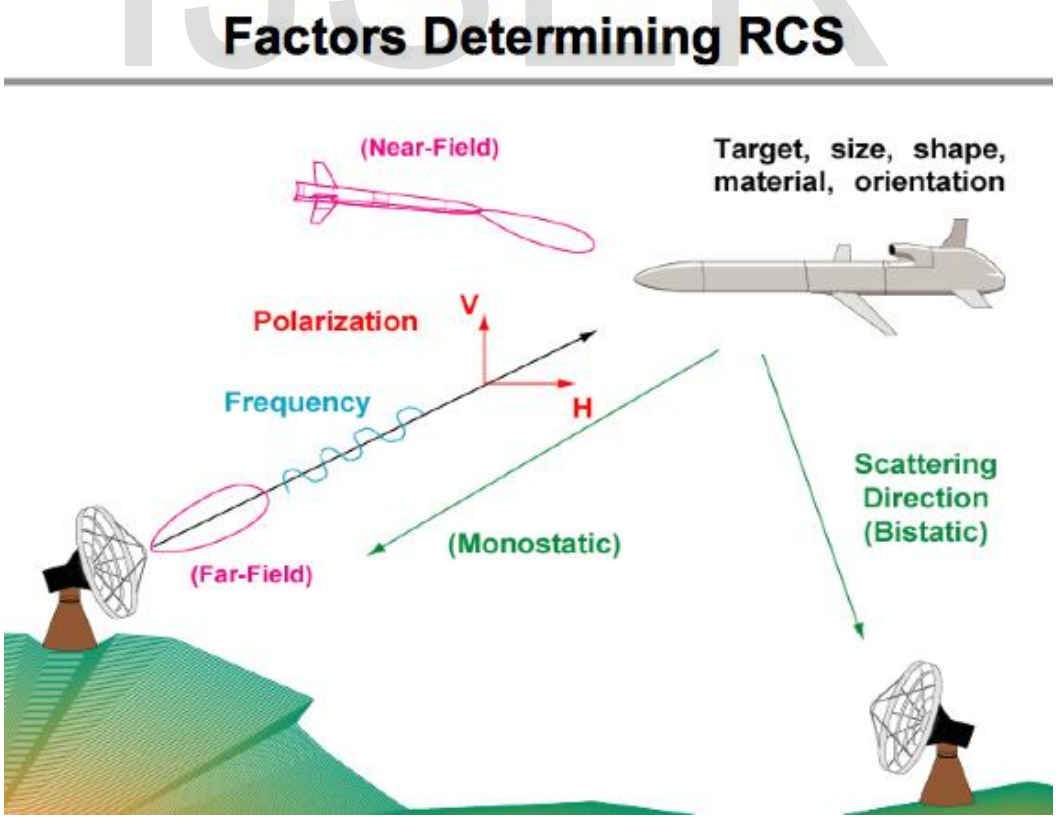

('Donnell and IEEE Aes Society, 2011)

3.2.1 Frequency of transmitted wave from radar

At a low frequency, the probability of detecting stealthy target is higher compared to when the radar is transmitting at a higher frequency; therefore the radar cross-section of a target is higher at a low radar frequency. This is why military air traffic control radar uses a low frequency band (L Band) so as to allow for maximum detection of stealth aircraft; L band frequency is typically between the ranges of 1 to 2GHz.

Air traffic control radar for civil aviation uses S-band frequency, which ranges from 2GHz to 4GHz. Most civil aviation radars use a frequency between 2.7GHZ to 2.9GHz, typically 2.9GHz (Butler and Johnson, 2003).

Relatively higher frequency is used in civil aviation radars compared to military radar in order to reduce the number of clutter that is generated from unwanted objects with relatively low radar cross-section like birds, rain droplets, but in the case of military air traffic control, having low frequency radar that can detect most stealth aircraft with relatively low radar cross-section is beneficial, however a powerful radar processing unit is required. (Butler and Johnson, 2003)

To understand how frequency affects radar cross-section, we will look at the calculation of the **radar cross-section of a flat square plate** with an area of $4m^2$;

At 2.2GHz, if the radar transmits normal to the flat surface, the plate will have a radar cross-section of $\sigma = 4\pi A^2 / \lambda^2$

Where σ=RCS, λ=wavelength and A=area.

At 2.2 GHz, wavelength λ=0.1363m (from λ=speed of light/frequency);

Speed of light = $(3X10^8 m/s)$

Thus RCS (σ) =10813m^2.

*Note: If the incident angle of the radar wave is not perpendicular (normal) to the target, some portion of the EMW energy may be reflected away from the radar receiver; hence, the above calculated radar cross-section magnitude changes.

Conversely, for a perfect electrically conducting sphere of cross sectional area $1m^2$; i.e. diameter equals 1.13 m, will have an RCS (σ) =$1m^2$ (See Figure 18)

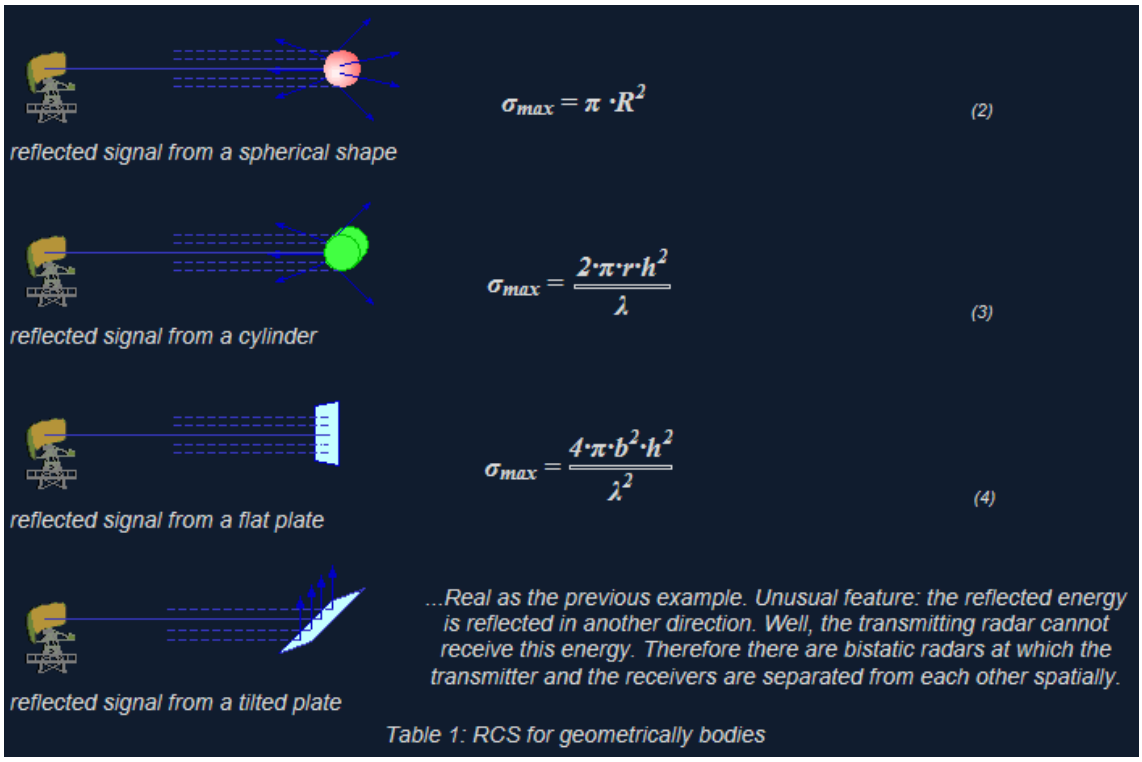

Figure 18 – Maximum radar cross section for simple perfectly electric conducting geometries. Dipl and Wolff, C. (2011)

3.2.2 Material of the target body

The reflectivity of a material also affects its radar cross-section; metals are highly reflective thus producing strong reflected signals. Most commercial air vehicles have metallic characteristic thus making them highly reflective, this allows them to be easily monitored by air traffic control radar.

Other materials such as wood, plastic have relatively low radar energy reflectivity thus making them suitable for radomes '*radomes are used to protect radar from adverse weather*'(Illustrated in Figure 19) and other low radar reflectivity applications.

Figure 19 - (Left) Uncovered radar, (Right) Radome covered radar (Military systems and technology, 2010)

On the other hand, some materials are specially designed to absorb radar energy, they are called Radar Absorbent Materials (RAM), they convert the electromagnetic energy of incident radar wave into heat energy, thus, ideally no energy is reflected back to the radar receiver; this in turns makes the radar cross-section of a target coated with RAM relatively low.

A number of military air vehicle makes use of RAM technology to effectively reduce radar cross-section.

3.2.2.1 Review of Radar Absorbent Materials

Since the development of radars, methods of reducing the reflected electromagnetic wave sent back to the radar receiver have been explored. Radar absorbers are sometimes classed as resonant absorbers. (Saville, 2005)

Resonant absorbers: This material is thin so that not all the radar wave power is absorbed. "This results in reflection and transmission at the first interface. The first reflected wave undergoes a phase reversal of π. The transmitted wave travels through the absorbing medium and is reflected from a metallic backing. This second reflection also results in a phase reversal of π before the wave propagates back to the incident medium" (Saville, 2005). This results in a destructive interference of the wave; hence reducing the intensity of the cumulative reflected wave. In cases where the magnitude of the two reflected waves is equal, the intensity of the total reflected wave is zero.

Radar absorbing materials are made from resistive and/or magnetic materials; they are design on **Ferrite based materials.**

Examples of radar absorbent materials include: Foam absorber, Iron ball paint, Jaumann absorber (Saville, 2005).

3.2.3 Shape of the target body

The characteristic shape of a target body is an important factor that contributes to its radar cross-section. It dictates the directivity of the body; that is, the direction in which radar energy is deflected. Where the surface shape is not flat, energy is concentrated in some direction and dispersed in other directions. The total radar cross-section of a target is not a constant value; it varies depending on the aspect angle of the target relative to the radar.

It should be noted that radar cross-section is not solely dependent on a target's cross sectional area, because if this was the case, the only way to reduce it RCS would be to make the physical structure of the target smaller. Alternatively, by absorbing or deflecting the radar energy away from the radar receiver, the target achieves a relatively lower radar cross-section.

In the same vein, the **scattering direction** of the incident radar energy is dependent on the shape of the target; hence the radar cross-section of a target also depends on the radar type. **Mono-static radar** has its transmitter and receiver in the same location, and a **Bi-static radar** has its transmitter and receiver in different locations, in a situations where the radar energy is reflected away from the source (transmitter) but towards the receiver in another location in the case of a bi-static radar; the radar cross-section detected is influenced.

To simulate the radar cross section of the wind turbine blade, a research into the capabilities of various available electromagnetic simulation software was carried out.

The following table is a decision matrix comparing various electromagnetic simulation software programmes.

Functional Considerations	Weighting Factor	CST MS	FEKO	Epsilon	ANSYS HFSS
Availability	**3**	3 x **3** = 9	1 x **3** = 3	1 x **3** = 3	2 x **3** = 6
Cost	**3**	3 x **3** = 9	2 x **3** = 6	1 x **3** = 3	2 x **3** = 6
Accuracy of output results	**3**	3 x **3** = 9	2 x **3** = 6	3 x **3** = 9	3 x **3** = 9
3D modelling capability	**2**	3 x **2** = 6	2 x **2** = 4	3 x **2** = 6	3 x **2** = 6
Total		**33**	19	21	27

(3 is Very Good, 1 is bad)

Figure 20 - Decision matrix comparing various electromagnetic simulation software programmes.

CST Microwave Studio scored the highest; hence this programme was used to run the radar cross-section simulation.

3.3 CST Microwave Studio

3.3.1 Critical evaluation of software

CST Microwave Studio (CST MS) is a software package used for the design and analysis of electromagnetic problems in the high frequency domain. It simplifies the process of creating structures by providing a graphical platform for solid modelling which is based on the ACIS modelling Kernel - this is a 3D modeller used in many CAD - Computer Aided Engineering, CAM - Computer Aided Manufacturing, Architecture applications. After the construction of model/structure, a fully automated process of meshing is applied prior to running simulation based on specified conditions such as frequency range, model material type. (Computer Simulation Technology, 2015)

CST Microwave Studio provides an environment to simulate problems individually; i.e., providing the best-suited approach to particular problems e.g. meshing type and solver type.

The major factor contributing to the output result is the solver type used during simulation; the solver types include: frequency domain solver, time domain solver, integral equation solver, asymptotic solver, multilayer solver and Eigen-mode. For the purpose of this project, the time domain solver was used during simulation of radar cross-section of the wind turbine blade as it provides flexible simulation capabilities. The time domain solver is able to obtain the behaviour of an entire broadband frequency in just one simulation run thus making it efficient. This solver uses a hexahedral mesh, based on FIT- Finite Integration Technique. (Computer Simulation Technology, 2015)

On the other hand, the integral equation solver was initially assumed to be the best option for the simulation of the wind turbine features as this solver is best suited for electrically large structure such as wind turbines, but the long simulation time taken to simulate problems using the integral equation solver presented a huge constraint.

The integral solver uses a volumetric discretization method; this however requires fine mesh to be created prior to simulation, the time taken to create these mesh cells is relatively long thus making the integral equation solver an unviable option for radar cross-section simulation of an electrically large structure like a wind turbine.

The time domain solver features useful for the purpose of this project include:

- An efficient and fast memory FIT-Finite Integration Technique (This provides quicker calculations compared to the integral equation solver)
- An efficient calculation for loss free and loss-structures (The importance of this is highlighted when simulating the proposed wind turbine blade with radar absorbent material)
- Supports more than two-billion mesh cells, but a 1:1 scale of the wind turbine blade will require mesh cells a lot more than two billion mesh cell, for this reason a **scaled model of 1:1000** of the original blade size was used during simulation to accommodate for this constraint. It should be noted that the behaviour of the radar cross-section of the scaled model is similar to that of a large sized turbine blade,

however radar cross-section magnitude will increase, but for analysis purposes the scaled model would be sufficient.

- Isotropic and anisotropic material properties.
- Antenna far field calculations- this includes calculations of side lobes suppression, gain, beam direction.
- Radar cross section calculation (Computer Simulation Technology, 2015).

3.4 Testing and simulation

3.4.1 Method

- To test the accuracy of the CST MS software, the total radar cross-section of a perfect electric conducting sphere of diameter 4cm was simulated in CST at 200MHz and compared to the manual calculations made using the formulas/ basic hypothesis governing RCS prediction(see Section 4.2).
- As illustrated in the 3D model in Figure 21, the wind turbine blade was modelled in solid works; and to make it compatible for simulation in CST MS environment, this part was converted to STL and imported into CST MS.
- The blade model was scaled down to accommodate for the simulation meshing constraint (1:1000).
- To ensure the output results are relevant in real world scenario, the simulation conditions corresponds to those used in civil air traffic control operations; these conditions include:
    - Frequency range: 2.7-2.9GHz
    - Simulation type: Bi-static scattering
    - Far field effects / Power loss calculation

This page is intentionally left blank.

Chapter 4

Analysis

Objective 4: Design and analyse the proposed solution

4.1 Modelling wind turbine in Solidworks

4.1.1 Wind turbine specification (GE 2015)

Type:

The widely used General Electric 1.5s-megawatt model

Blade length:

35.25m - For simulation purposes in CST, this was scaled down to 1:1000, which is≈ $0.03525m$

NACA:

This is the industry standard for aerofoil cross-section profile specification; **NACA 4415** was used for 3D modelling (Airfoil Tools, 2015)

Blade

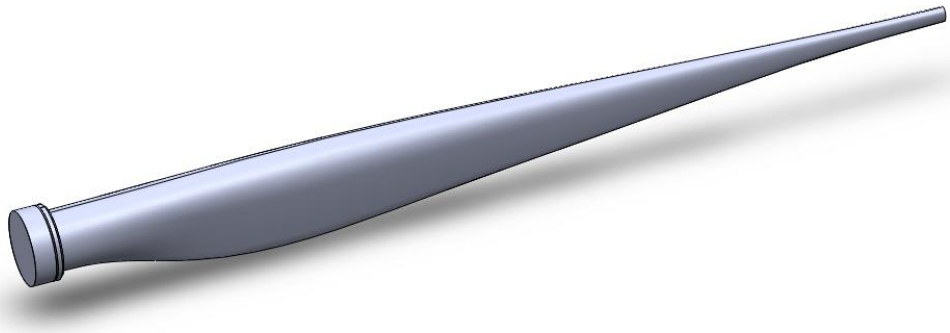

Figure 21 - Solidworks: 1:1000 NACA 4415 wind turbine blade

Tower, nacelle and hub

In this case, the tower, hub and nacelle are assumed to be a single feature, this is because the radar signature of these structures can be easily filtered out of the radar system; the

tower is a stationary target, so the Doppler filtering can be used (see Section 2.1 Understanding Doppler Effect), the nacelle shape can be varied to allow for reflectivity of radar waves away from radar receiver (see Section 3.2.3)

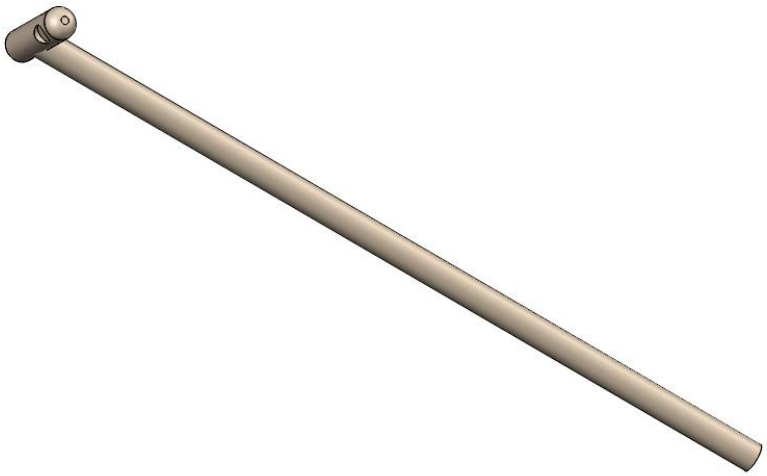

Figure 22 - Solidworks: Wind turbine tower and blade hub

Assemble 3-Bladed turbine

Figure 23 - Solidworks: Assembled 3-bladed horizontal axis wind turbine

*Note. The whole assembly of the wind turbine could not be simulated in CST due to the programme's limitation; i.e., its inability to create object interface mesh cells. The integral equation solver could simulate the STL format of the above assembly but as stated

previously, it takes a relatively long time to create mesh cells in the integral equation solver.

4.2 Software validation

4.2.1 Defining Terminologies

- Far-field:

This is a region far away from the transmitting antenna. The simulation was performed in a vacuum environment; thus radiation power loss as a result of weather condition is not taken into consideration.

- Lossy:

This describes a material that is less reflective of electromagnetic radiation e.g. radar absorbent materials

- Perfect electric conducting (PEC):

Reflects away all incident electromagnetic waves

4.2.2 Validation test

To test the validity and accuracy of CST, the antenna radiation pattern and radar cross-section prediction of a perfect electric conducting (PEC) sphere was simulated; a sphere provides a platform to validate the radar cross-section calculation made by the software.

According to Chapman & Hall/CRC (2000), the formulas used to predict radar cross-section magnitude are based on physical optics; hence the scattering of incident waveform on a perfect electric conducting sphere is categorized into three regions:

Optics region: This corresponds to a relatively large sphere; that is, where the radius of the sphere is much larger than the wavelength of the radar wave. Hence, the maximum radar cross-section of such sphere is governed by the equation

$$\sigma_{max} = \pi R^2;$$

Equation 2 - Optics region equation for the radar cross-section calculation of a PEC sphere

$$where\ \sigma\ is\ radar\ cross\ section\ in\ meter\ squared\ and\ R\ is\ the\ radius\ of\ the\ sphere(m)$$

In this region, the maximum radar cross-section of the sphere is independent on the frequency of the radar wave

$used\ when\ R \gg 10\lambda$ (Chapman & Hall/CRC, 2000)

Rayleigh region: This represents the region formed when the radar wave is at low frequency, that is, when the wavelength λ of the waveform is relatively larger than the target sphere (in the case of a relatively small sphere). The maximum radar cross-section of the sphere is governed by the equation

$$\boldsymbol{\sigma_{Max} \approx 9\pi R^2 \left[\frac{2\pi R}{\lambda}\right]^4}$$

Equation 3 - Rayleigh region equation for radar cross-section calculation of a PEC sphere

$where\ \sigma\ is\ radar\ cross\ section\ in\ meter\ squared\ and\ R\ is\ the\ radius\ of\ the\ sphere(m)$

$used\ when\ R \ll 10\lambda$ (Chapman & Hall/CRC, 2000)

Mie region: This represents scenarios where the radius of the sphere is comparable to the wavelength of the incident wave; this region is governed by a series of Maxwell's equations. A typical example of its application includes detecting of rain droplets with very high frequency (VHF) wave; the wavelength of the high frequency radiation is comparable to the radius of the rain droplet.

4.3 Radar cross-section prediction for a perfect electric conducting sphere in CST

- Wave frequency: 200MHz
- Sphere radius: 2cm

From the equation

$$\lambda = \frac{c}{f}\ where\ c\ is\ the\ frequency\ of\ light\ in\ a\ vacuum\ (3X10^8 m/s)\ and\ f\ is\ the\ frequency\ of\ the\ wave\ in\ Hz$$

Equation 4 - Wavelength formula

$$\lambda = \frac{300000000}{200000000} = 1.5m$$

From the above it can be seen that the wavelength λ is much larger than the 2cm (0.02m) radius of the sphere; hence radar cross-section calculations for this case will be governed by **Rayleigh's region** expression hypothesis.

$$\boldsymbol{\sigma_{Max} = 9\pi R^2 \left[\frac{2\pi R}{\lambda}\right]^4}$$

$$\boldsymbol{\sigma_{Max} \approx 9\pi \times 0.02^2 \left[\frac{2\pi \times 0.02}{1.5}\right]^4 = 5.57 \times 10^{-7} m^2}$$

Converting to logarithmic scale

$$\text{dBm2} = 10 \times \log_{10}(m^2)$$

Equation 5 - Radar cross section in meter squared to decibel square meter

Hence;

$$\boldsymbol{\sigma_{Max} \approx 9\pi \times 0.02^2 \left[\frac{2\pi \times 0.02}{1.5}\right]^4 = 5.57 \times 10^{-7} m^2}$$

$$\boldsymbol{\text{dBm2} = 10 \times \log_{10}(5.5 \times 10^{-7} m^2)}$$

$$\boldsymbol{= -62.54 dBm2}$$

Let now simulate the above sphere in CST MS environment

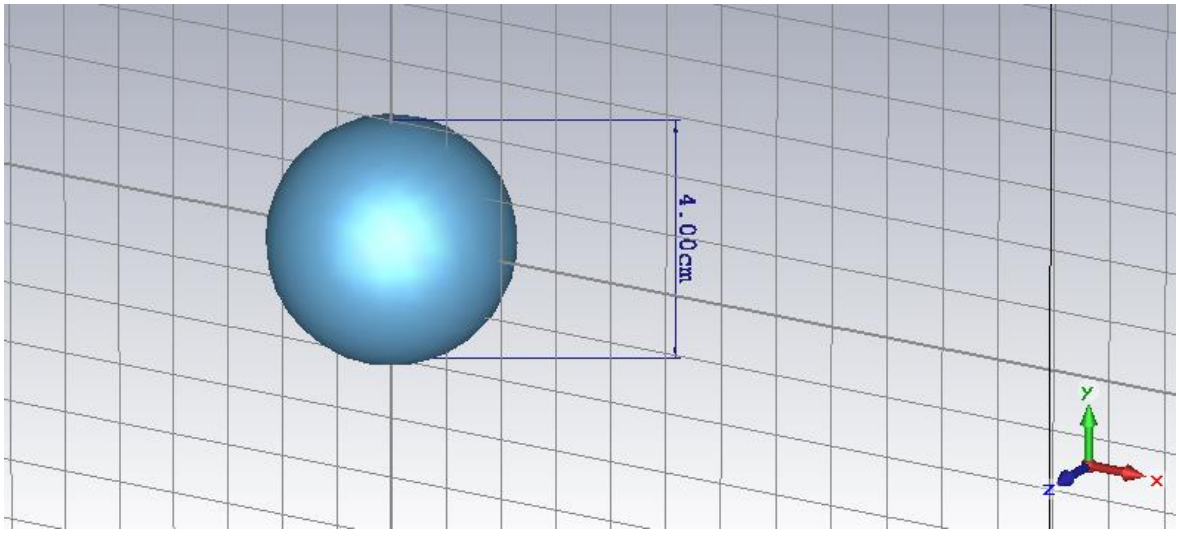

Figure 24 - CST 3D rendering of a perfect electric conducting sphere; radius 2cm

The simulation generates an antenna pattern to predict the maximum and total radar cross-section of the sphere at the specified frequency of 200MHz with an optimal angular beam width and radar position relative to the target (Sphere).

The angular width of the main beam is measured as the angular distance 3dB from the peak dBm2 magnitude of the main lobe (See Figure 25)

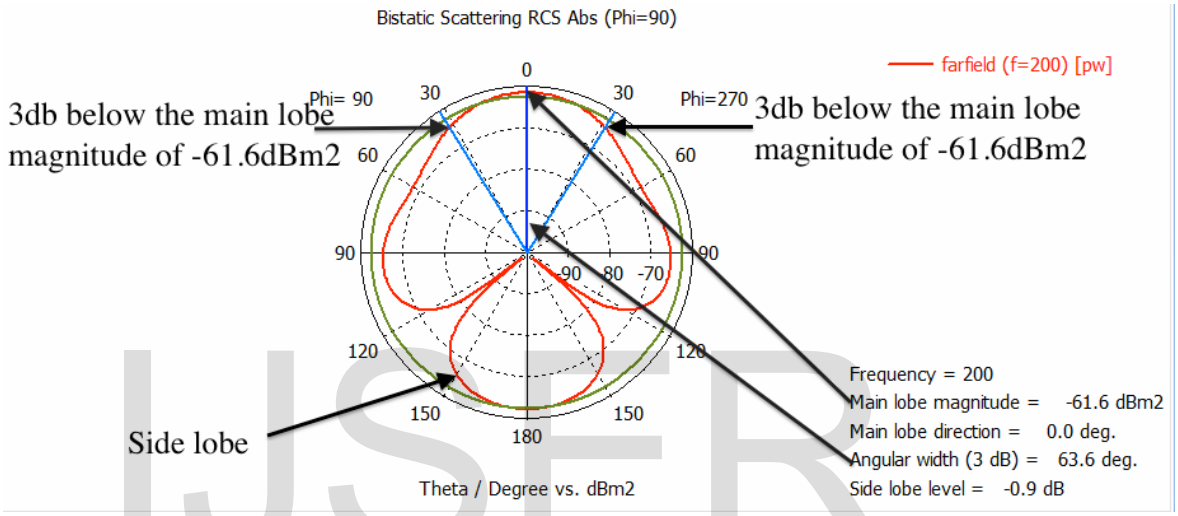

Figure 25 - CST: Antenna radiations (radar cross-section) of the sphere in logarithmic scale with respect to the azimuth/degrees about the antenna

The main lobe radiating at 0 degree has a magnitude of -61.61dBm2 and the other subsequent lobe is known as side lobe. Side lobes generally have radiation power level less than the main lobe; side lobes represent radiation in unwanted directions and radars are designed to have minimal side lobes, however this is most times inevitable.

4.3.1 Polar

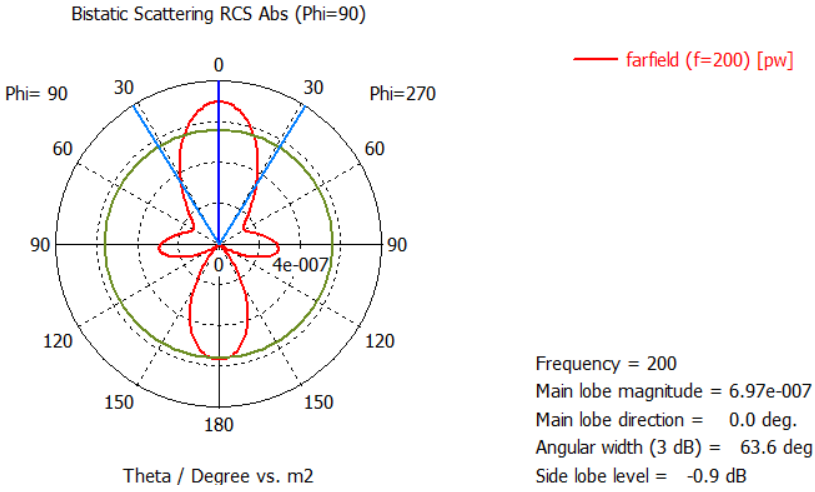

Figure 26 - CST: Linear scale of the antenna radiation (radar cross-section) in meter squared with respect to the azimuth/degree about the antenna

Detailed magnification of the above graph shows the maximum main lobe magnitude at -61.61dBm2, which corresponds to 6.97×10^{-7}m on the linear scale in Figure 28

From dBm2 $= 10 \times \log_{10}(m^2)$

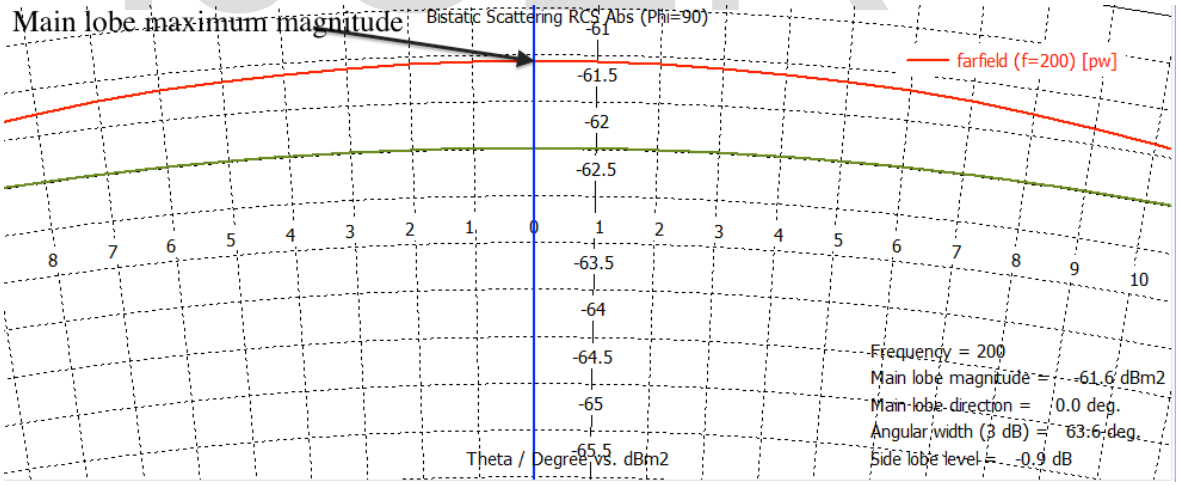

Figure 27 - CST: Maximum level of main lobe in logarithmic scale

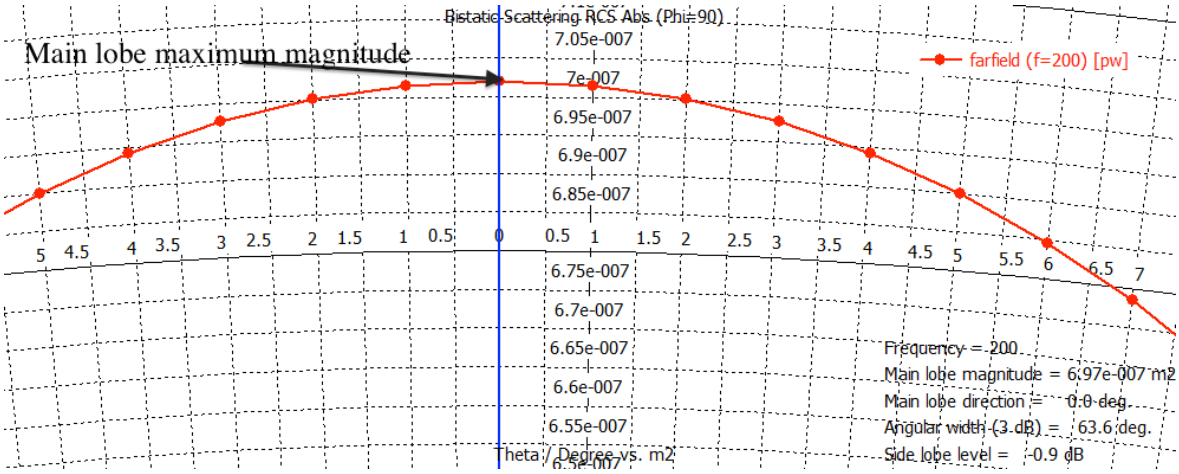

Figure 28 - CST: Maximum level of main lobe in linear scale

The total radar cross-section graph verses frequency provides information on how the total radar cross-section of the sphere changes with respect to frequency (Illustrated in Figure 29)

4.3.2 Total RCS

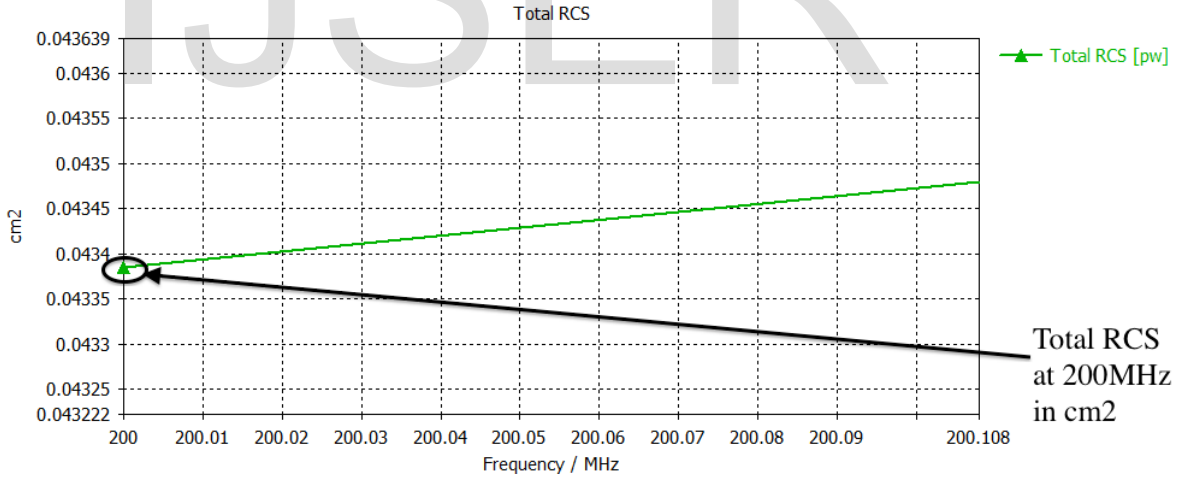

Figure 29 - CST: Graph of total radar cross-section in cm2 verses frequency in MHz

The value of total radar cross-section (Total RCS) at 200MHz in Figure 29 corresponds to the value in Figure 30

That is;

$$0.043356cm^2 = 4.34 \times 10^{-6}m^2$$

$$\text{dBm2} = 10\times\log_{10}(m^2)$$

$$\text{dBm2} = 10\times\log_{10}(4.34\times10^{-6}m^2) = -53.6dBm2$$

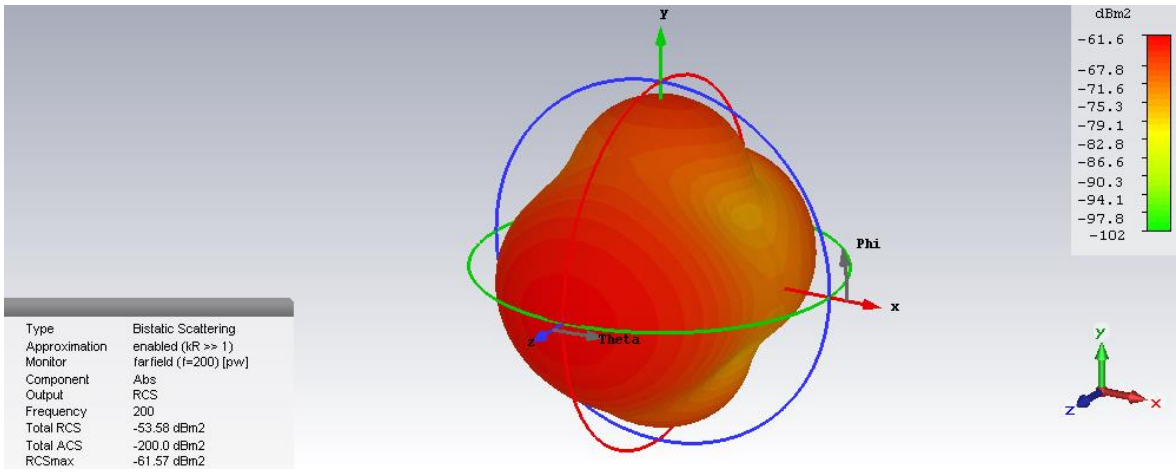

Figure 30 - CST: Maximum radar cross-section and total radar cross-section at 200MHz

In addition, the maximum radar cross-section recorded by the simulation as displayed above is **-61.57dBm2;** this is approximately ≈ $\boldsymbol{-62.54dBm2}$ as calculated from Rayleigh's region hypothesis previously.

From principle, the radar cross-section of an object is dependent on a number of factors as explained earlier (Section 3.2 Radar Cross Section (RCS); the analysis of the radar cross-section prediction of the PEC sphere of radius 2cm with incident wave frequency of 200MHz provided the expected result which corresponds to Rayleigh region physical optics theory.

In summary, this shows that CST MS simulation provides a valid radar cross-section prediction; thus enabling the simulation and accurate prediction of the radar cross-section of a more complex shape like the above wind turbine blade as required (Illustrated from Section 4.4 - 4.7 below).

4.4 Radar cross section simulation of a radar energy reflective wind turbine blade in CST

Objective 4.1: Model current conventional wind turbine blade and analyse its Radar Cross Section (RCS).

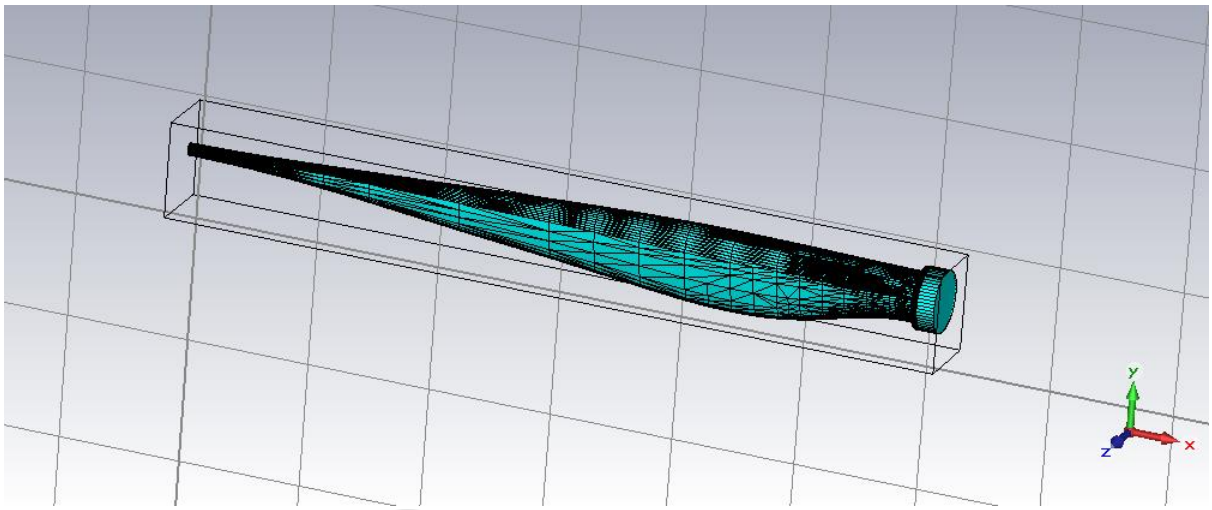

Figure 31 - CST: 1:1000 scale of a standard radar energy reflective wind turbine blade in CST environment (Specifications in section 4.1.1)

Following the same process as the sphere simulation in Section 4.3, the antenna generates an optimal antenna pattern in the XZ plane with the Z arrow being the reference corresponding to the direction of the peak of the main lobe.

4.4.1 Polar

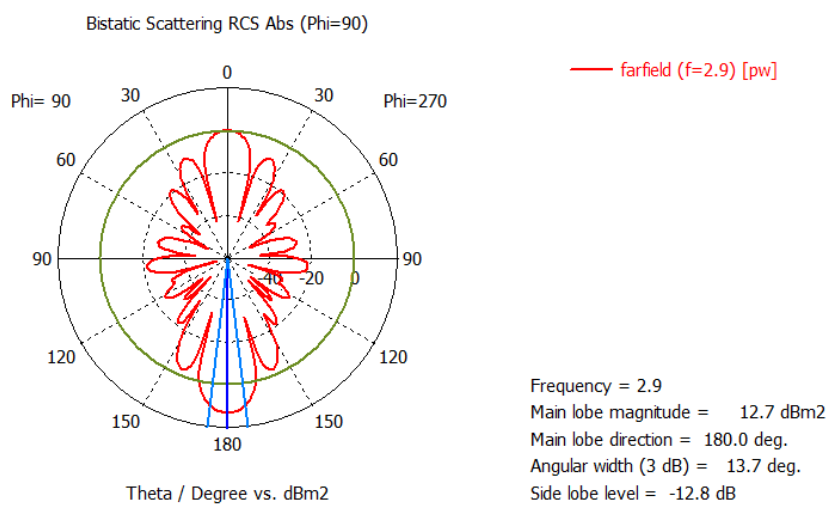

Figure 32 - CST: Antenna radiations (radar cross-section) of a reflective wind turbine blade in logarithmic scale (Polar coordinate) with respect to the azimuth/degree about the antenna

This shows the magnitude of the bi static scattering of the radar radiation with respect to azimuth/degrees around the transmitting radar/antenna.

4.4.2 Cartesian

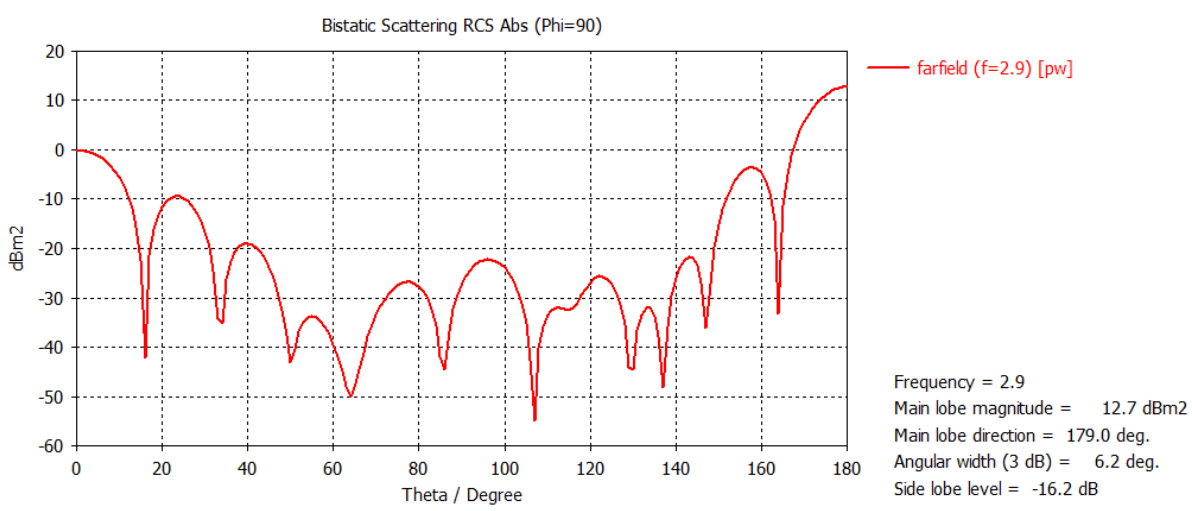

Figure 33 - CST: Antenna radiations (radar cross-section) of a reflective wind turbine blade in logarithmic scale (Cartesian coordinate) with respect to the azimuth/degree about the antenna

The Cartesian scale in Figure 33 provides a clear understanding of the polar graph in Figure 32. As illustrated, at 180 degrees, the magnitude of radar cross-section in both Figures corresponds to the value 12.7dBm2

4.4.3 Total RCS

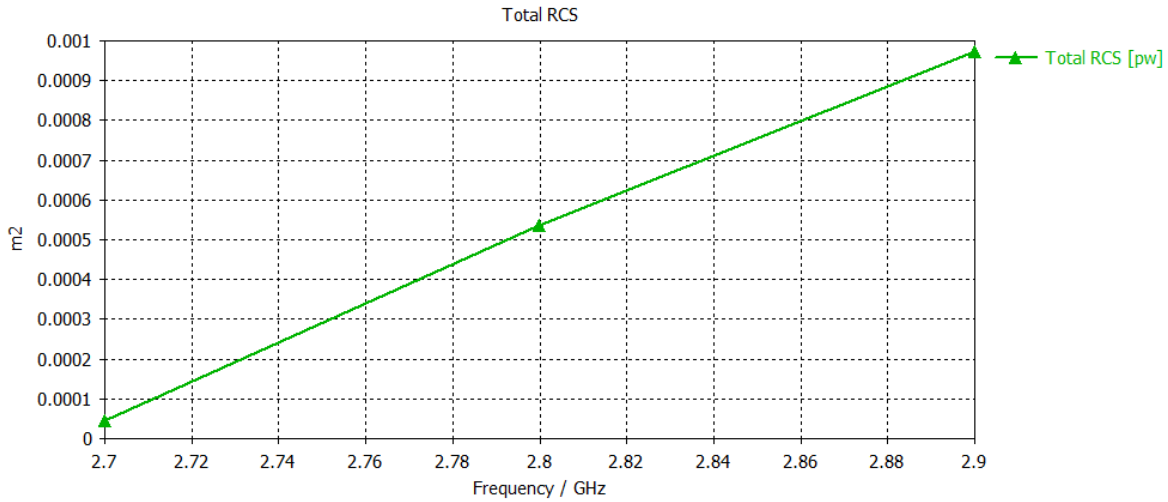

Figure 34 - CST: Graph of the total radar cross-section of the above radar reflective wind turbine blade in m2 verses frequency in GHz

This shows the total radar cross-section of the blade; as illustrated in Figure 34, the total radar cross-section increases with the increase in wave frequency; thus as stated previously, we notice that radar cross-section of a target is dependent on frequency of the incident radar wave. At the conditions highlighted in Section 3.4.1 - bullet point 4, this is the total radar cross-section at frequency ranging from 2.7 - 2.9GHz.

*Note: The material used during the simulation possesses similar properties as the one used by wind turbine blade manufacturers; that is, it is an electric conducting and a radar energy reflective material.

4.5 Aerodynamics of wind turbine

To reduce the total radar cross-section of the wind turbine blade, it was initially considered to reduce the effective surface area of the blade since target size contributes to the radar cross-section (see Section 3.2). However, doing this will result in the reduction in the lift, thus effective rotation generated by the blade at specific wind speeds, as lift is proportional to area (wind turbine blade size)

$$Lift = 0.5\rho A v^2 Cd$$

Equation 6 - Aerodynamic lift formulae

In the same vein, the area of a target is not the only contributing physical factor to radar cross-section; the direction in which the radar wave is reflected also plays an important role in the magnitude of radar cross-section a target produces.

According to QinetiQ, (2009) a slight change in the profile, structure and design of a turbine blade results in an immense difference in its reflective properties, effectively the radar cross-section magnitude. Hence, whilst changing the shape of wind turbine blades to allow for an effective scattering of radar wave away from the radar receiver may prove effective in mitigating wind turbine effects, this will in turn affect the amount of power generated by the turbine, as the turbines may not harness enough wind energy resulting in the wind turbine blades not rotating at a high speed enough to produce required power (AE-News, 2010)

Another possible technique that could be implemented is the change in the material the wind turbine blade is manufactured from.

Majority of stealth aircraft owe their stealth properties to the material of their chassis (B.C. and Norton, G.M., 2007). This method of making targets stealthy prompted the idea of simulating the same wind turbine blade design as in Section 4.4 with different materials in CST, i.e., implementing Radar Absorbent Materials (RAM) during the simulation. (See Section 4.6)

According to Carter, B.C. and Norton, G.M. (2007), the F117 Nighthawk implements the used of ferrite as its primary radar absorbent material; this is because its magnetic and electric conductivity properties makes it a good material for stealth applications.

*Note: From the knowledge of Doppler filtering (Section 2.1), the radar cross-section produced by a stationary object can be easily filtered out; thus any reflection produced by the wind turbine tower can be filtered out of the radar system because the tower is stationary; hence radar cross section simulation of the tower is not necessary for analysis purposes.

4.6 Radar cross section simulation of a wind turbine blade with radar absorbent properties

Objective 4.2 Model proposed wind turbine blade using stealth principles and analyse its radar cross section.

The simulation conditions is the same as in Section 3.4.1 - bullet point 4; however the wind turbine blade is assumed to be made of radar absorbent material (lossy) rather than a reflective material as in Section 4.4

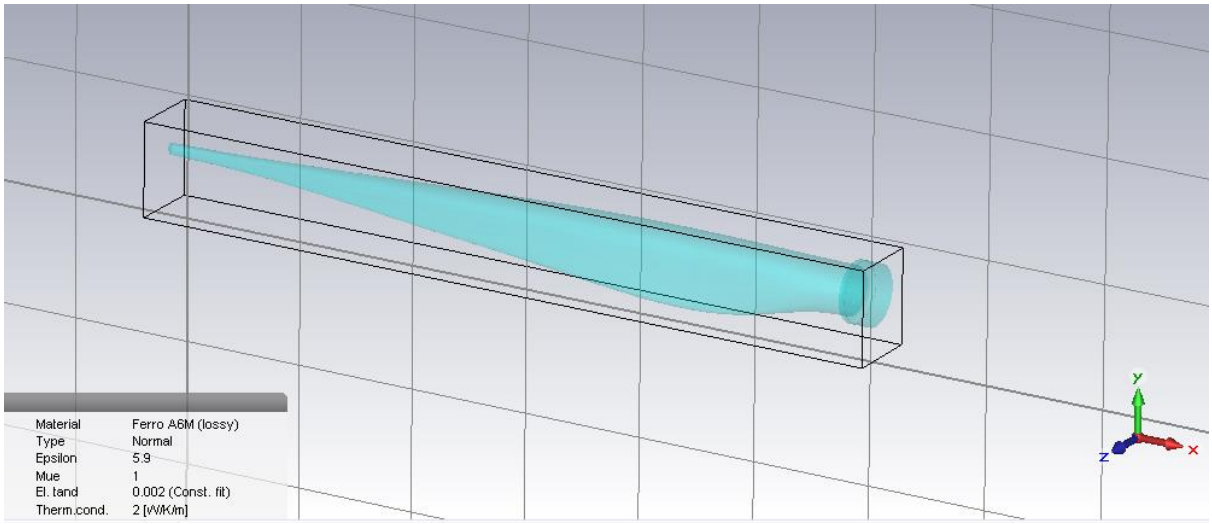

Figure 35 - CST: 1:1000 scale of a less reflective wind turbine blade with radar absorbent properties in CST environment

4.6.1 Polar

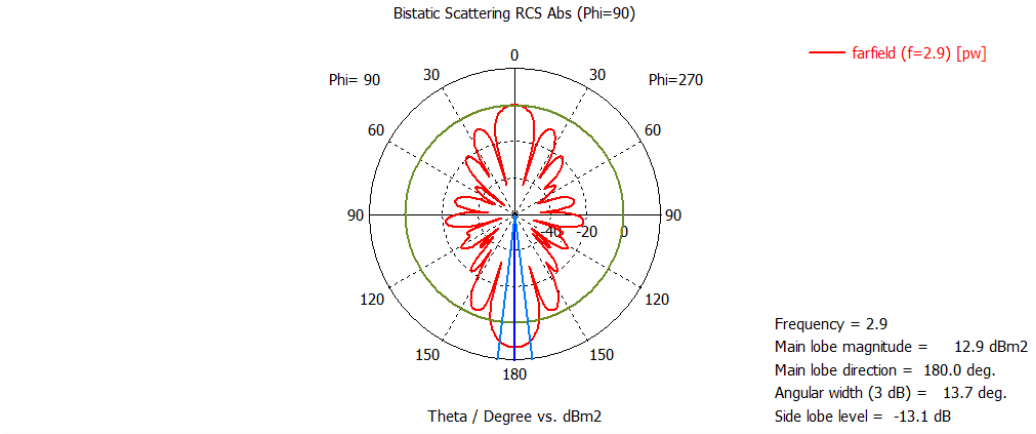

Figure 36 - CST: Antenna radiations (radar cross-section) of a less reflective wind turbine blade with radar absorbent properties in logarithmic scale (Polar coordinate) with respect to the azimuth/degree about the antenna

The radiation pattern in (Figure 36 above is the same as Figure 32) this is because the blade structure is the same in both simulations; hence the optimal radiation pattern used to predict the total and maximum radar cross-section of both cases, that is (Section 4.4 and Section 4.6) are the same, this is also important for RCS comparison purposes (Section 4.7)

4.6.2 Cartesian

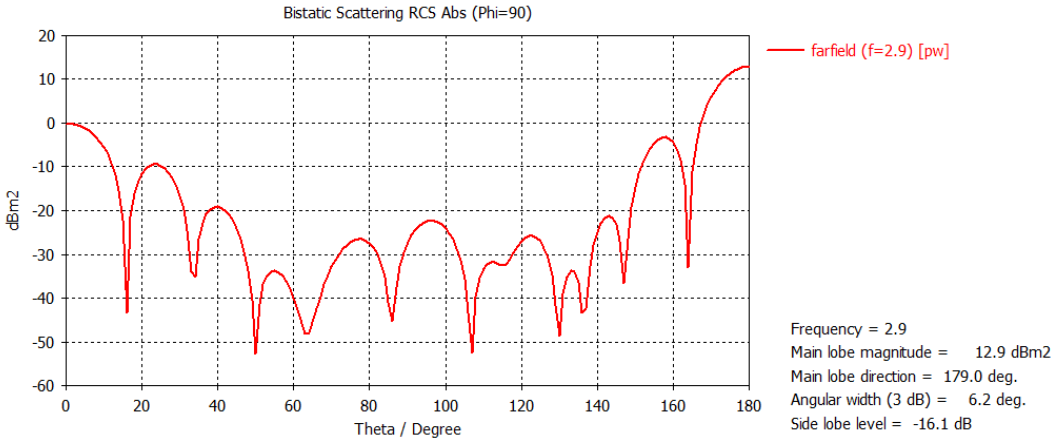

Figure 37 - CST: Antenna radiations (radar cross-section) of a less reflective wind turbine blade with radar absorbent properties in logarithmic scale (Cartesian coordinate) with respect to the azimuth/degree about the antenna

4.6.3 Total RCS

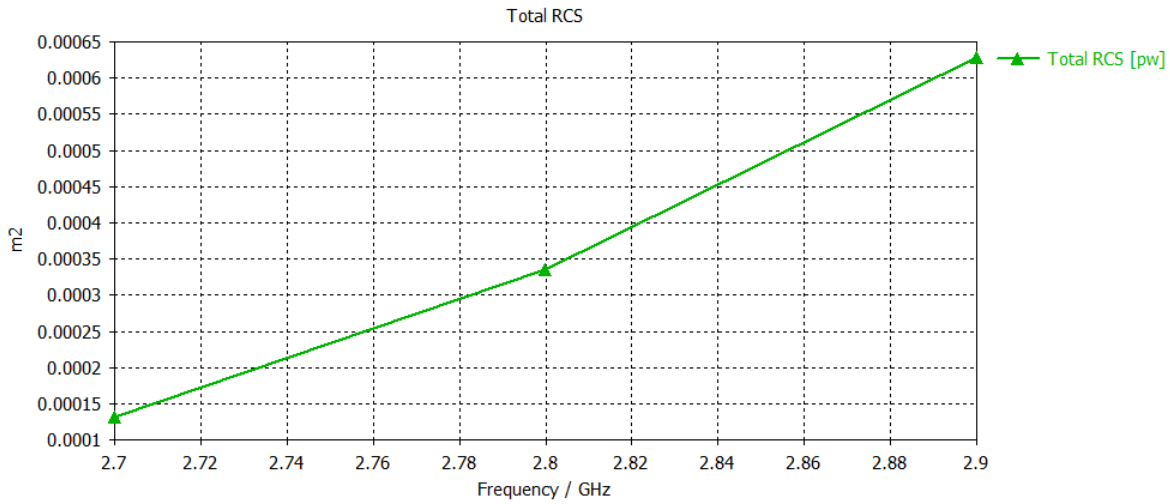

Figure 38 - CST: Graph of the total radar cross-section of the less reflective wind turbine blade in m2 verses frequency in GHz

4.7 Comparing RCS of reflective blade to stealth blade

Objective 4.3: Compare the RCS of the proposed stealth wind turbine blade to the conventional wind turbine blade.

The total radar cross-section of the blade as illustrated in Figure 38 above is slightly lower compared to the simulation in Figure 34 at the same frequency (0.001m2 in Figure 34 compared to 0.000625m2 in Figure 38 at 2.9GHz; i.e., in logarithmic scale, -30 dBm2 to -32.041dBm2 respectively).

Although the difference in total radar cross-section between the simulations in both cases is not extremely high, the slight difference in RCS highlights that implementing an improved radar absorbent material with better non-reflective properties than Ferro (Lossy), such as ferrite (International and Samuels, 1998) during manufacturing of a wind turbine blade would have greater effect in reducing radar cross-section of the wind turbine blade (see Section 3.2.2.1 for a review of how radar absorbent materials work)

*Note: Ferrite was not used during the simulation because it was not available within the software, the closest substitute with similar radar absorbent properties was Ferro (lossy).

Further research into radar absorbent types, properties as well as studying the feasibility of implementing radar absorbent materials during the manufacture of a wind turbine blade will be essential.

*Note: As illustrated in Equation 5, radar cross section in decibels with respect to 1 square meter is expressed as

$$dBm^2 = 10 \times log_{10} RCS\ in\ square\ meters$$

To put this to scale

$$60dBm^2 = 1\ million\ square\ meters$$

$$40dBm^2 = 10000\ square\ meters$$

$$20dBm^2 = 100\ square\ meters$$

$$0dBm^2 = 1\ square\ meters$$

$$-10dBm^2 = 0.1\ square\ meters$$

$$-20dBm^2 = 0.01\ square\ meters$$

4.8 Performance analysis of a wind turbine blade, considering factors such as its weight/material density

Objective 4.4: Analyse how the implementation of Radar Absorbent Materials (RAM) will affect the efficiency of a wind turbine blade.

Wind tunnel testing

Aim

Due to the unavailability of a RAM, the analysis conducted in this section is based on the assumption that the weight/density of a RAM will effectively be different from the conventional composite material 'fibre glass, carbon fibre' used to manufacture majority of the wind turbine blades currently in place.

With this assumption, this section presents a wind tunnel testing set up and also analyses the performance of two pairs of wind turbine blades, each with the same size and profile but different weight.

*Note: The weight difference was achieved by 3D printing one pair of the blades with 10% material infill and the other pair with 100% material infill

Set up

- Two pairs of the blades (Figure 45) were 3D printed each pair with different weight; 13g and 8g pair.
- The 13g pair and 8g pair were tested individually for performance analysis (RPM, current, voltage generated by the individual pair of blades).
- To begin the test, the wind tunnel environment was analysed in order to determine and adapt the environment to mount the wind turbine blades for testing.
- A motor from a drill was removed and adapted unto the mount to record the performance parameters during testing (see Figure 53 for mount design specification).
- The root of the blade was modified to allow for anchorage on the mount (Figure 45).
- At specific air velocities for the different blades (13g and 8g), the following performance parameters were measured; RPM of the blade, current, voltage using a tachometer, ammeter and voltmeter respectively.
- The circuit diagram in Figure 47 illustrates how the parameters were measured.

Results

Airspeed (m/s)	RPM of motor (radians/second)	Ampere (mA)	Voltage (V)	Power (mW)
14.4	17.90707813	0.021	7	0.147
17.5	26.38937829	0.031	10.15	0.31465
20.9	34.55751919	0.041	13.15	0.53915
23.8	42.14970144	0.051	16.13	0.82263
27.5	50.68436148	0.06	19.41	1.1646

Figure 39 - Reading from the test conducted with 13g blades

Airspeed (m/s)	RPM of motor (radians/sec)	Ampere (mA)	Voltage (V)	Power (mW)
14.4	27.96017462	0.033	10.82	0.35706
17.5	38.85102915	0.046	14.84	0.68264
20.9	50.73672136	0.06	19.17	1.1502
23.8	62.83185307	0.074	21.5	1.591
27.5	74.76990516	0.083	25.8	2.1414

Figure 40 - Reading from the test conducted with 8g blades

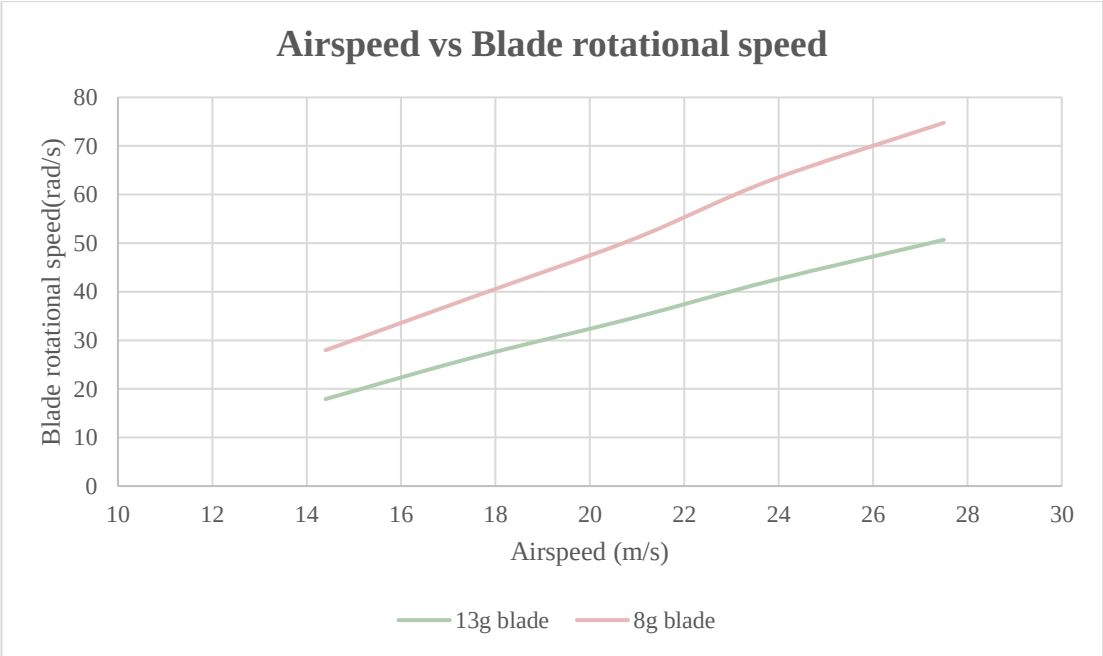

Figure 41- Graph comparing the rotational speed of the 13g and 8g blades at different airspeeds

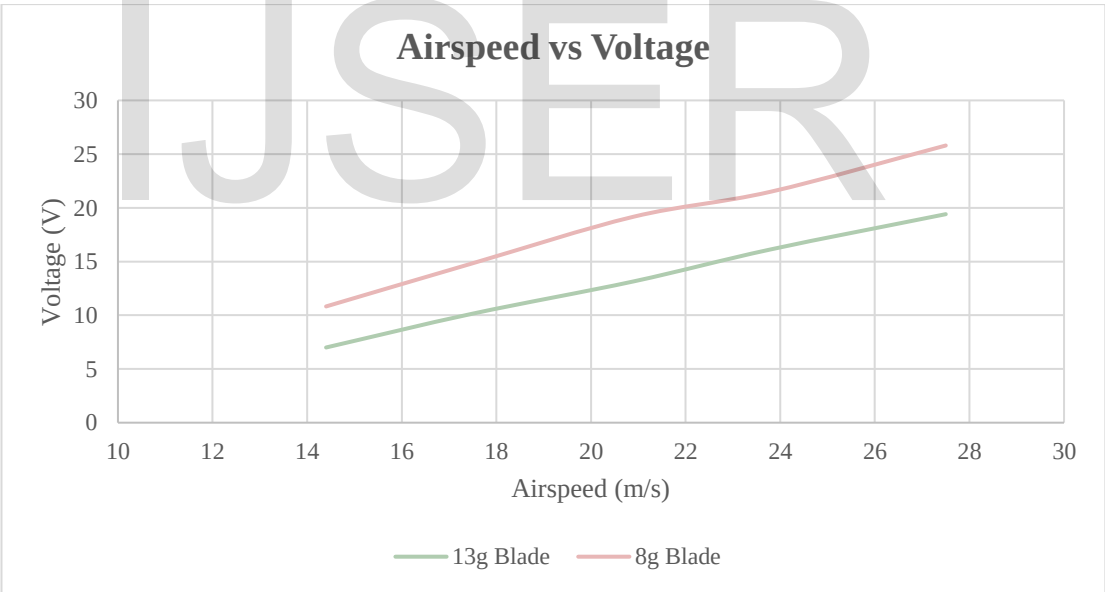

Figure 42 - Graph comparing the voltage generated by the 13g and 8g blades at different airspeeds

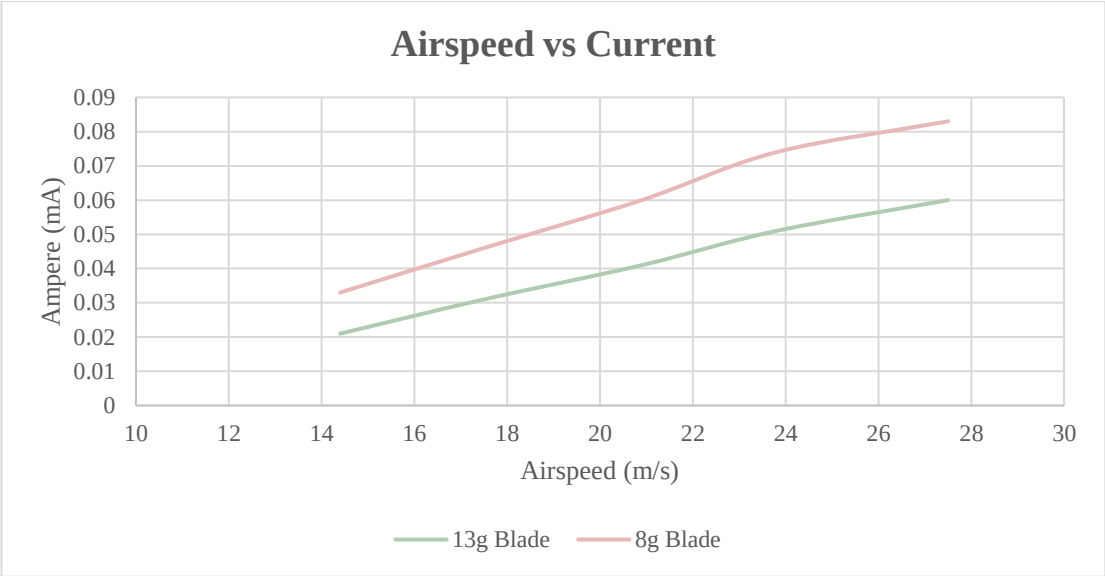

Figure 43 - Graph comparing the current generated by the 13g and 8g blades at different airspeeds.

Figure 44 - Graph comparing the power generated by the 13g and 8g blades at different airspeeds.

The results from the wind tunnel testing above shows that a slight increase in the weight of the wind turbine blade significantly reduces how much power the blade generates. Hence, before manufacturing wind turbine blades with RAM, it is essential to evaluate how much excess weight this may result in.

This page is intentionally left blank.

Chapter 5

Evaluation of results: Conclusion

The aim of the project was to investigate what initiatives should be undertaken in order to mitigate the effects wind turbines have on air traffic control. The entirety of this project has been based around the objectives highlighted below.

Furthermore, the summaries of the findings with regards to the individual project objectives are as follows:

Objective 1: Identify what the cause of the issue is and investigate the current solutions.

As highlighted in Chapter 2, the main effects wind turbines pose on air traffic control is that they are interpreted as aircraft due to the large RCS as well as Doppler effects produced by the wind turbines, this Doppler effect is comparable to that produced by an aircraft; hence, the wind turbines appear on the radar screen as a false aircrafts which in turns pose unwanted clutter thus making the effective tracking of real aircraft difficult. Various mitigation measures have been implemented from radar technology advancements to wind farm developments objection but they have not been effective in tackling this problem.

Objective 2: Identify the areas that are currently affected by the presence of wind turbines

The satellite image above in Figure 15 shows the vast dispersion of wind farms across the UK, the magnitude of the problem caused by these wind farms is immense, and hence, today any wind farm development project that is perceived to have a potential effect on air traffic control services is being opposed/halted. This has resulted in a tremendous amount of potential wind energy projects to be stopped (Chapter 2 Section 2.2.2). As highlighted in the table in Figure 14, of 10.69GW of wind generated electric power being held, 2.2GW contributes to objections made by air traffic control and as the demand for electric power is ever increasing, opposing wind farm developments is not a viable solution to this issue.

Objective 3: Propose an alternative mitigation measure, identify its practicality and determine its applicability and implementation.

After understanding the scope of the current mitigations in place, a proposed mitigation, which is the development/manufacture of wind turbine blade using stealth material as explained in Chapter 3.1 was made. This prompted the analysis of how stealth materials, that is, how radar energy absorbent materials affect the magnitude of the radar cross-section of the wind turbine blade.

Objective 4.1: Model current conventional wind turbine blade and analyse its Radar Cross Section (RCS).

To ensure the delivery of objective 3, the wind turbine blade was modelled in Solidworks and analysed in CST MS (see Section 3.3 to understand the capabilities of CST MS); however to ensure the results CST MS simulation produced were valid, the basis for radar cross section calculation was explored.

A sphere which is relatively a simple shape to manually calculate radar cross section was simulated in the CST MS environment, after the radar cross section result was produced, it was analysed and compared against the underlying principle governing radar cross section which is 'physical optics' (Equation 2 and Equation 3). The values CST MS produced for the radar cross section of the sphere corresponded to the values from the calculations made using the basic hypothesis and equations for calculating radar cross section.

After validating the software programme, the radar cross section of a conventional wind turbine blade was simulated, the values were analysed and compared to the simulation in Section 4.6.

Objective 4.2: Model proposed wind turbine blade using stealth principles and analyse its radar cross section.

Using the same conditions as the simulation of the conventional wind turbine blade, the same wind turbine blade was simulated with the addition of a stealth material. The radar cross section produced was slightly lower than that of the conventional wind turbine blade, this showed that implementing radar absorbent material, that is, materials with low radar reflectivity, aids the reduction of the radar cross section of a wind turbine blade.

Objective 4.3: Compare the RCS of the proposed stealth wind turbine blade to the conventional wind turbine blade.

The slight change in radar cross-section difference between both cases (Section 4.7) will be much larger in real life scenario this is because the simulated models were scaled down

to 1: 1000 (see Section 3.4.1). The small change in radar cross section is also due to the fact that ferrite - a standard radar absorbent material used in stealth aircraft was not available within the software for simulation. Simulating with an improved radar absorbent material like ferrite other than the *Ferro (Lossy) - a close substitute* used during this simulation will result in a large difference in radar cross section magnitude.

Objective 4.4: Analyse how the implementation of Radar Absorbent Materials (RAM) will affect the efficiency of a wind turbine blade.

From the results shown in Section 4.8, it can be said that implementing RAM during the development and design of wind turbine blades will involve wind turbine developers to consider the amount of additional weight this will result in. This is because a slight increase in the weight of a blade significantly affects the power the blade generates.

Objective 5: Provide recommendation on what the best mitigating measure is using data from the above analyses.

From the research and analysis presented in this report, the current mitigations (Chapter 2) in place although beneficial in the short term are not sufficient, therefore, the future of wind farm radar mitigation could lie in the development of stealth wind turbine blades; **if this area is explored by the wind farm industry it could provide a long term solution to this issue.** However, the feasibility of its implementation, that is, the engineering capability as well as the cost-benefit of implementing this mitigation method is unknown; this is an area that will require further work.

This page is intentionally left blank.

Chapter 6

Suggestions of further work

6.1 Effects of radar absorbent materials on wind turbine blade efficiency

- An extensive analysis of the effects of Radar Absorbent Materials (RAM) have on wind turbine blade efficiency will present a platform to base decisions as to how feasible it is to implement RAM into the design and manufacture of wind turbine blades. This was initially set as part of the objectives of the project; however, after a background research, it was revealed that the materials that are needed to perform this analysis are unavailable.

6.2 Mie region analysis

- Calculation and prediction of radar cross section in the Mie region; analysis of the series of Maxwell's equations governing radar cross section prediction in this region; that is, simulating a target with comparable radius to the wave length of incident wave (see Section 4.2.2). This will be needed for a more rigorous validity test of CST MS or whatever software used to perform the RCS simulation

6.3 Limitations

- Unavailability of '*Epsilon-A tool used for radar cross-section prediction'* to perform more rigorous radar cross section calculations. Acquisition of Epsilon will allow for more flexible simulation such as radar cross section prediction at higher frequency domain as well as RCS prediction of a full scale wind turbine.
- In this project, the wind turbine blade model was scaled down in other to simulate its radar cross section due to CST MS inability to create mesh cells for a relatively large full scale wind turbine blade. Simulation of a full scale model of a wind turbine blade would be essential for further analysis of radar cross section magnitude.
- Simulating the radar cross section of wind turbine components (blades, nacelle and tower) as a whole; CST MS is not capable of processing the assembled parts due to its difficulty in generating meshes at interferences. In the same vein, the wind

turbine as a whole was too large to be processed by CST MS; simulating a fully assembled wind turbine would be essential for further analysis.

This page is intentionally left blank.

Chapter 7

Project Management

To ensure the successful delivery of the project within the given time frame, the project was managed using a structured Gantt chart (See Appendix). The project management plan was detailed in the Gantt chart; it was produced at the beginning of the project, the project deliveries with reference to the Gantt chart were met within the required time frame.

Some of the project objectives were further broaden or streamlined in some cases to align with the project aim after a background research was carried out into the respective subject area. Re-evaluations of project plan were made whenever the need arose.

The project planning process on a whole was very effective, thus ensuring the successful delivery of the project within the specified deadline.

Reference

AE-News (2010) *Increasing the efficiency of wind turbine blades*. Available at: http://www.alternative-energy-news.info/efficiency-of-wind-turbine-blades/ (Accessed: 11 February 2016).

Airfoil tools (2015) Available at: http://airfoiltools.com/ (Accessed: 14 December 2015).

Barton, D.K. (2004) *Radar system analysis and modeling, volume 1*. Available at: https://books.google.co.uk/books?id=dvlPAwAAQBAJ&pg=PA91&lpg=PA91&dq=rayleigh+region+small+sphere&source=bl&ots=JyghIWjafH&sig=iMM3sy_pmg8KTw4NgLYJulqDaa8&hl=en&sa=X&ved=0ahUKEwj-0Om-9O3KAhVJvxQKHcImA9MQ6AEIJzAE#v=onepage&q&f=true (Accessed: 11 February 2016).

Bevelacqua, P. (2009) *Beamwidths and Sidelobes: Radiation pattern definitions*. Available at: http://www.antenna-theory.com/basics/radPatDefs.php (Accessed: 9 February 2016).

Butler, M.M. and Johnson, D.A. (2003) *FEASIBILITY OF MITIGATING THE EFFECTS OF WINDFARMS ON PRIMARY RADAR*. Available at: http://users.ece.utexas.edu/~ling/EU1_Feasibility_Mitigating_Effects_Windfarms_on_Primary_Radar_Butler_Johnson_UK.pdf (Accessed: 13 February 2016).

CAD library (2012) Available at: https://grabcad.com/library/f-117-nighthawk-stealth-fighter-1 (Accessed: 12 February 2016).

CAP 670: *ATS safety requirements* (2014) Available at: http://publicapps.caa.co.uk/modalapplication.aspx?appid=11&mode=detail&id=200 (Accessed: 12 February 2016).

Carter, B.C. and Norton, G.M. (2007) *Ceramic materials science and engineering*. New York: Springer.

Chapman & Hall/CRC (2000) *Radar cross section (RCS)*. Available at: http://dsp-book.narod.ru/RSAD/C1828_PDF_C02.pdf (Accessed: 10 February 2016).

Computer Simulation Technology (2015) *CST MICROWAVE STUDIO-Workflow and Solver Overview*. 1st edn. .

Defense-Aerospace (2014) *Stealth technology: Theory and practice*. Available at: http://www.defense-aerospace.com/articles-view/feature/5/157481/aircraft-stealth%3A-the-view-from-russia.html (Accessed: 12 February 2016).

Dipl and Wolff, C. (2011) *Radar basics - radar cross section*. Available at: http://www.radartutorial.eu/01.basics/Radar%20Cross%20Section.en.html (Accessed: 9 February 2016).

'donnell, Robert M O and Ieee Aes Society (2011) *IEEE new Hampshire section radar systems course 1 radar cross section 1/1/2010 radar systems engineering lecture 7 – part 1 radar cross section IEEE new Hampshire section guest lecturer*. Available at:

http://ece.wpi.edu/radarcourse/Radar%202010%20PDFs/Radar%202009%20A_7%20Radar%20Cross%20Section%201.pdf (Accessed: 14 February 2016).

ECHO (2006) Available at: http://echoincontext.mc.duke.edu (Accessed: 14 February 2016).

Feko (2010) *Radar Cross-Section (RCS)*. Available at: https://www.feko.info/applications/RCS (Accessed: 25 October 2015).

Fleseriu, F. (2014) *LP ELECTRIC wind turbine diagram*. Available at: http://www.lpelectric.ro/en/support/wind_diag_en.html (Accessed: 14 February 2016).

Frolic, K. (2013) *Radar line of sight assessment (online)*. Available at: http://www.pagerpower.com/news/goole-fields-wind-farm-little-john-in-fill-radar-solution/ (Accessed: 14 February 2016).

General Electric (2015) *Wind*. Available at: http://www.ge.com/in/wind-energy/ (Accessed: 14 December 2015).

Hays, P. (2014) *Talos missile guidance and homing history*. Available at: http://www.okieboat.com/History%20guidance%20and%20homing.html (Accessed: 21 November 2015).

Hodgkins, L. (2009) *Schoolphysics:Welcome:* Available at: http://www.schoolphysics.co.uk/age14-16/glance/Waves/Doppler/index.html?PHPSESSID=43cdadeaf8c0a5aeacf88cced9468bab (Accessed: 14 February 2016).

International, A. and Samuels, L.E.E. (1998) *Light microscopy of carbon steels*. United States: ASM International.

LCDR Brent J. Flaskerud (2006) *Detection theory*. Available at: http://www.usna.edu/Users/physics/ejtuchol/documents/SP411/Chapter19.pdf (Accessed: 12 February 2016).

Military systems and technology (2010) Available at: http://www.militarysystems-tech.com/military-gallery (Accessed: 13 February 2016).

NATS (2015) *Wind farms*. Available at: http://www.nats.aero/services/information/wind-farms/ (Accessed: 21 November 2015).

O'Donnell, R.M. (2002) *Introduction to radar systems*. Available at: http://ocw.mit.edu/resources/res-ll-001-introduction-to-radar-systems-spring-2007/ (Accessed: 14 February 2016).

Oyelaja, H. (2015) *How wind farm pre-planning assessment is carried out*. Available at: https://vimeo.com/143498454 (Accessed: 12 February 2016).

Panda, A. and Diplomat, T. (2014) *How effective is china's new anti-stealth radar system, really?* Available at: http://thediplomat.com/2014/10/how-effective-is-chinas-new-anti-stealth-radar-system-really/ (Accessed: 13 February 2016).

P and Galloway, E.R. (2001) *Radar signatures and relations to radar cross section*. Available at: http://www.roke.co.uk/resources/papers/Radar-Signatures-and-Relations-to-RCS.pdf?q=resources/papers/Radar_Signatures_and_Relations_to_RCS.pdf (Accessed: 9 February 2016).

Pike, J. (no date) *Military*. Available at: http://www.globalsecurity.org/military/world/stealth-aircraft-rcs.htm (Accessed: 14 February 2016).

Pollitt, M. (2016) *A new generation of turbines*. Available at: http://www.theguardian.com/technology/2009/aug/19/micro-wind-power-turbines (Accessed: 14 February 2016).

QinetiQ (2009) *QinetiQ and Vestas claim world first in radar mitigation wind turbine technology*. Available at: http://www.qinetiq.com/media/news/releases/Pages/stealth-turbine-trial.aspx (Accessed: 11 February 2016).

Radar concepts | ECE 480 team 5*: Interactive radar demonstration* (2014) Available at: http://www.egr.msu.edu/classes/ece480/capstone/spring12/group05/radar.html (Accessed: 14 February 2016).

RenewableUK (2015) *The voice of wind & Marine Energy*. Available at: http://www.renewableuk.com (Accessed: 21 November 2015).

Robert, D. (2005) *RES.LL-001 Introduction to Radar Systems*. Available at: http://ocw.mit.edu/resources/res-ll-001-introduction-to-radar-systems-spring-2007/ (Accessed: 21 November 2015).

Saville, P. (2005) *Review of Radar Absorbing Materials*. Available at: http://dtic.mil/dtic/tr/fulltext/u2/a436262.pdf (Accessed: 21 November 2015).

Techxplore (2014) *France to build wind farm with stealth turbine blades*. Available at: http://techxplore.com/news/2014-09-france-farm-stealth-turbine-blades.html (Accessed: 12 February 2016).

Set up

Figure 45 - Wind turbine blades (13g pair) mounted on the motor for wind tunnel testing

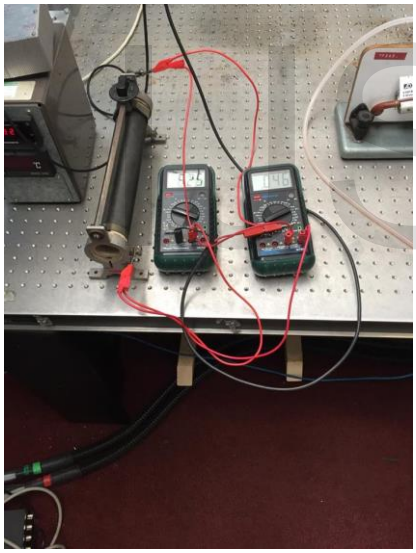

Figure 46 - Voltmeter, ammeter and resistor (4ohms) used for recording performance parameter (see Figure 47 for circuit diagram)

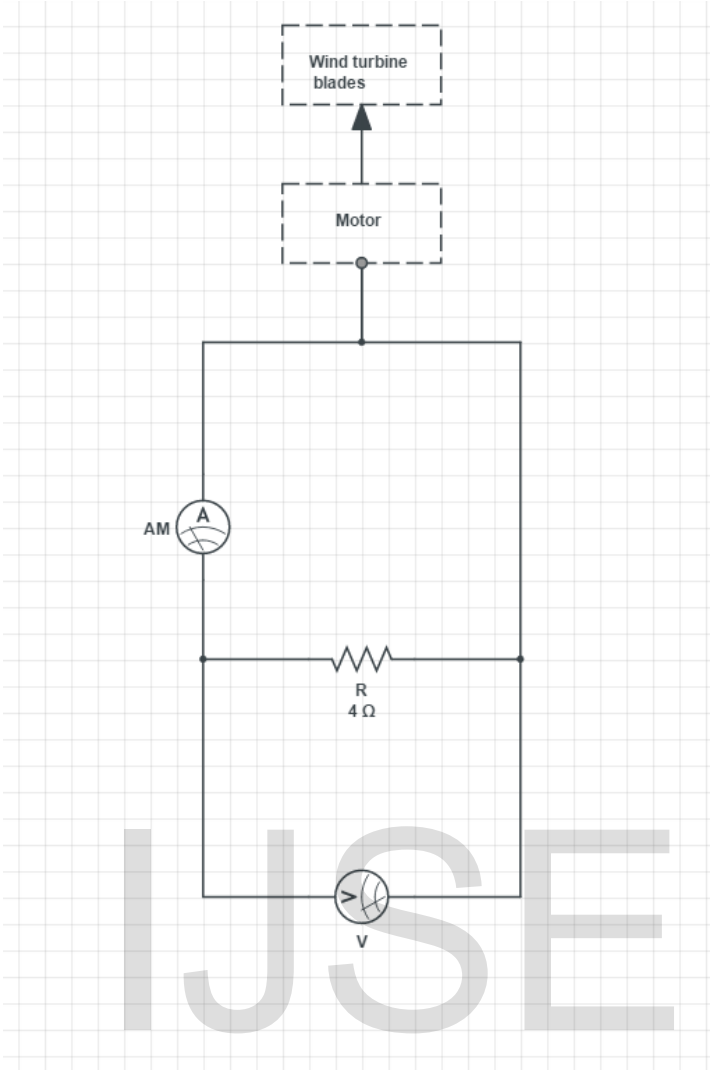

Figure 47 - Circuit diagram for measuring the electrical performance parameters of blade

Manufacture of wind turbine model for project exhibition day

The wind-turbine parts consists mainly of scrap materials, manufactured parts or purchased complete parts; these parts were assembled in the University of Brighton laboratories. The blades are a smaller scale of the wind tunnel model; the ends were modified in Solidworks to allow for attachment to the nacelle.

Figure 48 - 3D printed wind turbine blade model

Figure 49 - Solidworks model of wind turbine model

Figure 50 - Assembled wind turbine blades attached to hub

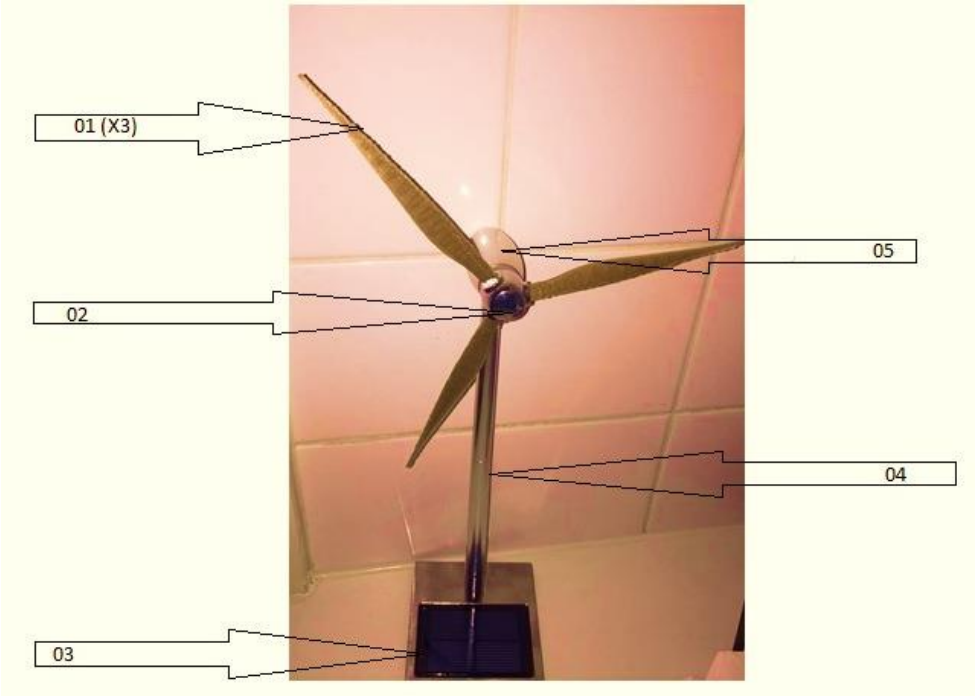

Figure 51 - Balloon labelled parts of assembled wind turbine

Parts list

Item number	Item description	Quantity	Supplier
01	Wind turbine blades (PLA)	3	Manufactured using 3D printer in the University of Brighton's lab
02	Blade hub	1	Scrap RC helicopter blade hub
03	Solar panel	1	Alibaba.com 'Bespoke'
04	Hollowed aluminium rod	1	Alibaba.com 'Bespoke'
05	Motor Housing/ Motor	1	Alibaba.com 'Bespoke'

Figure 52 - Parts list of assembled wind turbine

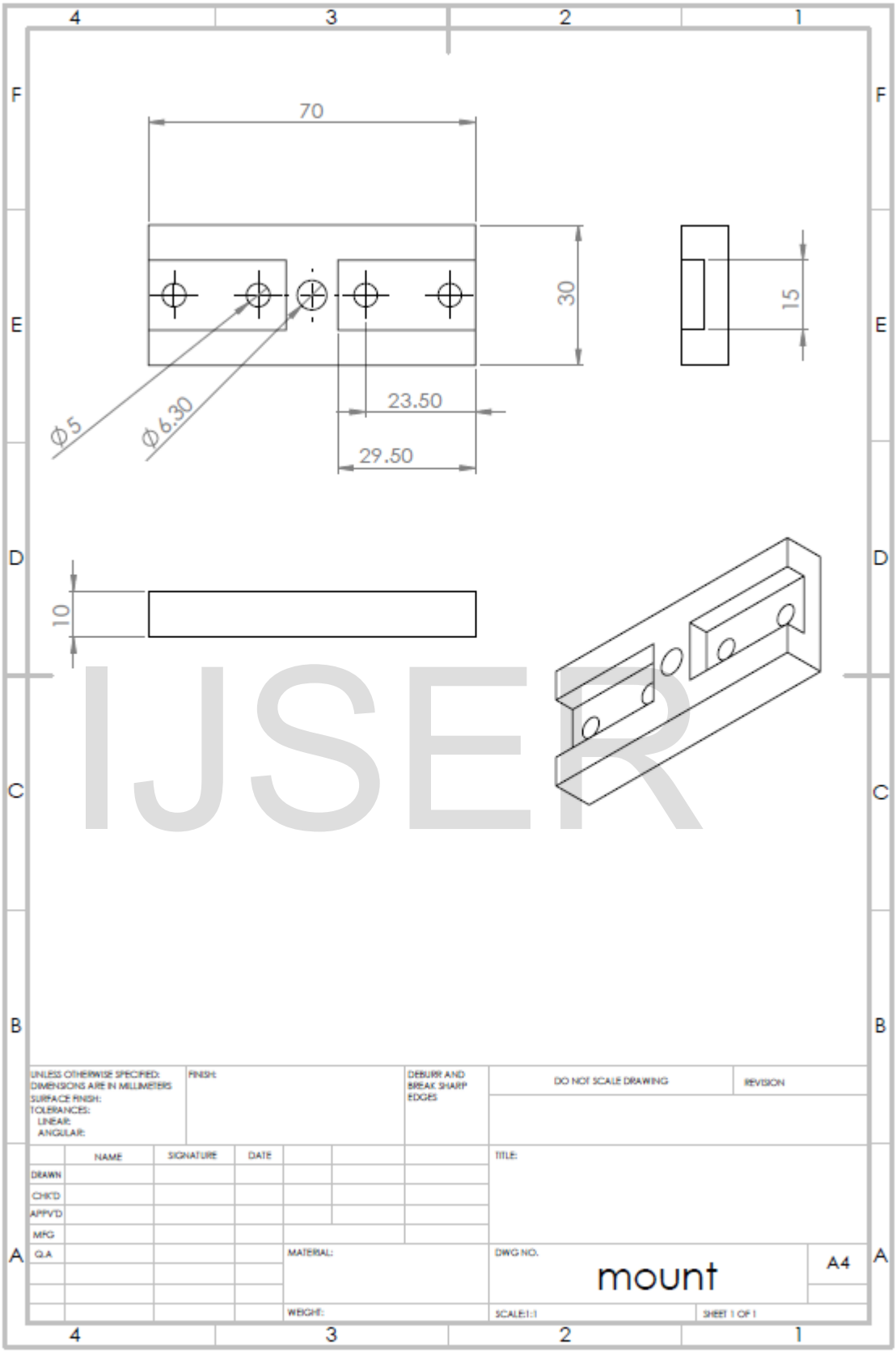

Figure 53 - Mount in First angle projection